MATHEMATICS DEPARTMENT

LAMINAR NATURAL CONVECTION IN A RECTANGULAR CAVITY

PRESENTER: THOYA, PATRICK KITSAO
B.ED (Hons.)

SUPERVISOR: GATHERI, FRANCIS KIMANI
(Ph.D.)

A project submitted in partial fulfillment of the requirement for

Degree of

MASTER OF SCIENCE

OF

SCHOOL OF PURE AND APPLIED SCIENCE

KENYATTA UNIVERSITY

JULY 2002.

TABLE OF CONTENTS:

ABSTRACT

This project is basically a numerical study of the structure of the flow and heat transfer rates due to collision of opposed laminar natural convection boundary layer in an enclosure.

Natural convection plays an important role in the flow and heat transfer in a wide range of technological applications. A fluid motion of a Boussinesq fluid in a three dimension rectangular cavity has been considered. To enable the analysis of flow and heat transfer rates, a complete set of non-dimensionalsed equations governing newtonian fluids and boundary conditions were recast into vorticity/vector potential to eliminate the need for solving the continuity equation.

The governing equations with the boundary conditions were discretised using a three-point central difference approximation for a non-uniform mesh. The resulting finite difference equations were then solved using the method of false transients and the Samarskii-Andreyev. A powerful computer code was used to generate the current results. The non-uniform mesh has been implemented in the project to allow for efficient use of computer time and storage. This enables placement of more nodes in regions of high velocity gradients and fewer nodes in other regions so that the total number of nodes used is minimized. This mesh type does not compromise

the accuracy of the solution as it is demonstrated that order o(h^2) accuracy may be maintained, where h is the spatial step size. The Rayleigh number used to obtain the current results was between 5×10^5 and 5×10^6. The study revealed that at higher Rayleigh number, there is substantial increasing exchange of hot air from the lower region to the upper region and vice versa. Temperature tends to decrease as the flow moves away from the 'active wall'

DEDICATION

To my son Bright

ACKNOWLEDGEMENT

I am greatly indebted to my supervisor, Dr.Francis Kimani Gatheri, who has tirelessly inspired me in undertaking this work. The completion of this project has been mainly due to his timely encouragement, and surely has left an impression, which will continue to influence my future research work .I will always remember you.

Much thanks also goes to all lecturers of Mathematics department for their cooperation, which made it possible for me to complete the program on time. I extend thanks to my father Mr Jonathan Maitha, my mother Mrs Josphine Maitha, my brothers: Benson, Justine, and Adam, my sisters: Patience, Irene, Santa, Dorine,Kadzo and Maridadi, for their love, understanding and prayers and for patiently enduring the many sacrifices as a result of this project.

I am also sincerely gratefully to my cousin, Onesmus (fudhi) for his tireless encouragement at times when things seemed not to be moving. Thank you for being there at the right time. Special thanks goes to my wife Jacqueline Benjamin for giving me all the encouragement and peace of mind to undertake this course within the time required. You surely made an impact to this project Finally I would like to thank The almighty God for his mighty care and concern for me.

NOMENCLATURE

Roman symbols

x	x-coordinate in the i^{th} direction
y	y-coordinate in the j^{th} direction
z	z-coordinate in the k^{th} direction
u	velocity in the x-direction
v	velocity in the y-direction
w	velocity in the z-direction
T	Thermodynamic Temperature
t	Time
u*	Characteristic velocity
p	Thermodynamic pressure
Ra	Rayleigh number
Re	Reynolds number
Pr	Prandtl number
Pn	Pressure number
S	Specific entropy
l_x l_y l_z	Length of cavity in the x, y and z directions.
L	Characteristic length.

$E_1,\ldots..,E_3$ Dimensionless parameters.

n coordinate normal to boundary.

$C_1,\ldots..,C_6$ Coefficients used in finite difference approximations to first and second derivatives.

g Acceleration due to gravity.

N_x, N_y, N_z Total number of mesh points in the x,y,and z directions.

h Heat transfer coefficient

Greek Symbols

α Thermal diffusivity

$\alpha_\theta, \alpha_\zeta, \alpha_\psi$ False transient factors.

β Coefficient of volumetric expansion.

γ Angle between two vectors.

∇ Gradient operator

Δt Time internal

δ_{ij} Kronecker delta

δ_x, δ_{xx} Central difference operators denoting the first and second partial derivatives in the x-direction.

$\zeta_1, \zeta_2, \zeta_3$	Vorticity in the x, y and z direction.
θ	Non-dimensional temperature.
μ, μ_s	First and second coefficient of viscocity respectively.
ρ	Density.
σ	Weighting factor.
λ	Thermal conductivity.
τ	Viscous stress tensor
Π	Stress tensor.
Φ	Dissipation function.
ϕ	General variable.
ψ_1, ψ_2, ψ_3	vector potential in the x, y and z direction.
ω	Intermediate variable used in the ADI scheme.

Subscripts

b	Boundary value.
C	Cold wall.
i,j,k	Denotes the i^{th},j^{th} and k^{th} mesh point in the x,y and z directions respectively.
R	Reference state.

Superscripts

n	Current time step.
n 1	New time step value.
*	Intermediate value in the ADI scheme.
/	Fluctuating or dimensional quantity.

Abbreviations:

ADI	Alternating Direct Implicit.
FDE	Finite Difference Equations.
FFT	Fast Fourier Transform
GGDH	General Gradient Diffusion Hypothesis.
H.O.T	Higher Order Terms.

CHAPTER ONE

1.1 Introduction

A fluid is a substance which continuously deforms under the action of slight shear force. Fluid dynamics is concerned with the study of the motion and condition that affect the motion of the fluid. Fluid kinematics, which deals with the forces involved in the motion, and fluid dynamics, which deals with the state of the fluid motion are the two types of fluid mechanics. Basically heat transfer is by conduction, convection, and radiation. In convection, an essential first step in the treatment of problem is to determine whether the boundary layer is laminar or turbulent because surface friction and the convection transfer rates depend strongly on which of these conditions exists. The scope of this project is on the laminar boundary layer. In natural convection, the driving force for the fluid motion is the gravity field acting on density difference as a result of differences in temperature boundary conditions. This situation creates buoyant force causing denser parts of the fluid to move downward and less dense parts to move upwards. Natural convection plays an important role in the flow and heat transfer in atmospherical, oceanographical and geophysical processes in nature as well as in a wide range of technological applications. In particular, convection phenomenon due to buoyancy driven flow inside a closed enclosure (i.e.

internal flows) subjected to differential heating is encountered in many practically important engineering problems. This include: thermal insulation of buildings, heat transfer through double windows, cooling of electronics equipment, general circulation of planetary atmosphere, sterilization of canned foods, cooling fluids in channels surrounding a nuclear reactor core, among others.

The study of free convection in the past decade focused mainly on two different simple geometry, first the single isothermal or constant flux vertical plate in isothermal stagnant surrounding, secondly the enclosed rectangular cavity with heated and cooled walls. The former flow is of parabolic character and can be handled comfortable by numerical method while the latter is of elliptic character which has to be converted to parabolic before solved. There are two flows in any enclosed cavity i.e. Double glazing "window cavity problem" in which two opposite vertical walls are differentially heated, and the Rayleigh-Bernard problem where opposite horizontal walls are heated and cooled.

Due to elliptic nature of internal buoyant flows, natural convection flows require a complete solution of the Navier-Stokes equations coupled with the energy equation.

Most of the fluid dynamics problems involving natural convection could be solved by experimental, theoretical and numerical method.

The experimental method would involve construction of a model in a laboratory and the measurement of various parameters (e.g. temperature and pressure) taken while the experiment is being conducted. The major drawbacks of this method is that it is expensive and time consuming.

The theoretical method requires analytical solution of the equations governing fluid motion. The drawback to this approach is that the mathematical theory required to solve the non-linear equations in their general form is still not clear. This is because the Navier~Stokes equations (the momentum equations) and the energy equation governing the phenomenon are highly nonlinear, and coupling between the boundary layer and the core region in the internal flows creates mathematical difficult in obtaining analytical solution.

The development and use of computational methods for numerical solution of the Navier-Stokes equations have been under way for more than five decade, but it is only in the last decade that notable contributions in the numerical simulation of fluid flows have been made. Among these, the most important one is the basic understanding of the relationship between the physics of the problem and the numerical procedure employed for its

solution. Basically numerical methods using digital computers are commonly utilized to solve a wide variety of flow problems. Although differential equation that govern the flow of Newtonian fluids (the Navier-Stoke equations) were derived many years ago, there are few known analytical solutions to them. With the advert of high-speed digital computers, it has become possible to obtain approximate numerical solutions to these (and other fluid mechanics) equations for a wide variety of circumstances. Of the various techniques available for the numerical solution of the governing differential equations of the fluid flow, the following three types are most common: (1) the Finite Difference method (2) the Finite Element (or Finite Volume) method, and (3) the Boundary Element method. The finite difference method for computational fluid dynamics is perhaps the most easily understood and widely used of the three above in predicting low-Rayleigh number natural convection. In this method the equations of motion are discretizing and marched through time until steady state is achieved. This gives complete control over all fluid properties such as viscosity and density and creates great flexibility in the choice of flow parameters such as the Rayleigh and Prandtl numbers.

In the following section, an overview of relevant literature in numerical and experimental studies concerning natural convection will be presented.

Emphasis shall be on internal flows in geometry heated and cooled from a vertical wall.

1.2 Literature Review on Natural Convection

1.2.1 Introduction

A wide range of problems in physics and engineering are concerned with the phenomenon of natural convection. Not surprisingly, it is attracting a large and expanding research effort both experimentally and numerically. For example the 1980 review of the heat transfer literature, lists 72 papers on confined natural convection alone, almost as many as were cited on channel flow. Eckert (1980).

Although in reality, fluid flow is three-dimensional, most numerical studies of natural convection in enclosed cavities were mostly restricted to two-dimensional flows and low Rayleigh number. A classical test problem in numerical heat transfer is the study of natural convection heat transfer in the enclosed, differentially heated square cavity.

Analysis of this simplified problem not only does it provide a sound basis for comparison of numerical approach but also the possibility of gaining physical insight into other related problems of practical interest. Both numerical and experimental studies have been carried out for natural

convection in fluid flow. Some researchers such as Eckert and Carsol (1961), Myneth and Duxbury (1974) and Brigs and Jones (1985) experimentally studied laminar and steady state flows.

A wide range of numerical investigation on the problem has been presented with different methods by researchers such as Wilkes and Churchill (1966) , Schmidt *et al.* (1970) and Le Quere (1990). Comparison research on the problem was presented by de Vahl Davis and Jones (1983) and Behnia *et al.* (1988), The total computing cost (CPU time usage and memory requirement) of different methods which was considered by the later, while the former considered mainly the accuracy of the numerical solution obtained by various researchers using different techniques.

Ostrach (1988) presented a review of the literature on internal natural convection flow in various geometries with different types of boundary condition as well as a section of the scale analysis. Gebhart *et al* (1988) presented a literature overview of the work on buoyant induced flows.

A comprehensive literature review concerning laminar natural convection in two-dimensional enclosure had earlier been written by Ostrach (1972) and Catlon (1978).

Similarly a number of researchers modeled a number of turbulent flows near vertical isothermal walls (isoflux) in their investigation. These include

studies by Mason and Seder (1974), Cebecci and Khattah (1975), Thomas and Al Sharif (1975), Plumb and Kennedy (1984), Humprey(1986) and Sigey (1998). These studies resulted in a better understanding of turbulence in natural convection boundary layers.

During the NATO-ASI conference in 1984 a number of subjects were given priority for further research in the future,(Kayac et al 1985). These include: high Rayleigh number natural convection was identified as one of the main subjects of future research, improvement in the existing numerical techniques, extension to three-dimensional calculations for practicality and real life situations and need for additional research on both laminar and turbulent modeling and wall functions as well as experimental validation of the numerical simulations, was considered to be of prime importance.

Following this development, Hoogendoon (1986) dedicated part of the review research paper on natural convection in enclosures to high-Reyleigh number turbulent natural convective flows. He considered in particular the relationship between experimental and numerical studies on one hand and the practical application on the other hand.

In general, natural convection in an enclosure arising from localized heating and cooling is encountered in a number of practical importance, such as use of convectional heaters in a room. In a room, besides forced convection,

natural (free) convection plays an important role in the determination of the indoor climate. The temperature and velocity fields in a room depend mainly on the temperature of any heat sources and windows as well as air ventilation flow rate.

1.2.2 Natural convection in an enclosure with localized heating and cooling

Natural convection is observed as a result of the motion of the fluid due to density changes arising from heating process. A hot radiator used for heating a room is one example of practical device, which transfers heat by free convection. The movement of the fluid in free convection results from buoyancy forces imposed on the fluid when its density in the proximity of the heat-transfer surface is decreased as a result of the heating process.

The buoyancy forces are due to some external force field such as gravity and do give raise to free convection. They are termed as body forces.

The problem of free convection in an enclosure has been much studied both experimentally and numerically., and comprehensive review is given by Schinkel (1980). Despite all this effort a clear overall picture of the processes involved as a function of the Prandtl number , Rayleigh number and Aspect ratio has yet to emerge. The importance of Prandtl number in

determining the type of flow was established by Elder (1978) for high Prandtl fluids such as oils and through the prediction of Jones (1982) for the low Prandtl numbers typical of liquid metals.

Humprey and Bleinc (1985) studied an enclosure composed of conducting vertical walls with the upper half cooled and lower half heated using the experimental method.

Yuon-sinh-luh (1988) carried out a numerical computation to investigate the underlying mechanisms contributing to the formulation of vertical structure in the flow that jets away from the wall. The studies concluded that the longitudinal structures were caused by the Rayleigh Bernads instability under the action of shear. The buoyant instability associated with the horizontal unstable stratified jet was the main contribution to the formation of longitudinal rolls. The size of the rolls is determined by the local condition i.e. the Rayleigh number and the Richardson Number in the horizontal jet, and in turn the local condition is determined by the temperature imposed on the conducting wall. Basically the longitudinal rolls are expected to form and disappear in a short distance from the conducting walls.

Poulikakos and Filis (1986) and Poulikakos (1985) presented both experimental and theoretical studies of free convection in an enclosure with

vertical wall, which could be heated on the top -half and cooled on the bottom- half. The results showed that when the temperature of the upper conducting plate is higher than that at the lower conducting sidewall, then there will only be a large horizontal vertical structure with axis parallel to the conducting sidewall. This became a clear indication that the flow structures observed by Humprey and Bleinc (1985) were as a result of collision process (centrifugal instabilty) of the horizontal jet from the wall.

Recent years have seen a number of both experimental and numerical studies of natural convection in building. Scale models have been used by a number of researchers such as Euser *et al.* (1978) Oslon and Glicksman (1991) ,Sanjurto and Cooper (1991) and Cooper and Kulkarni (1993). Other studies have been carried out in which a hot boundary layer interacts with a cold downward stream from a cold surface (Ellis and Glickman 1987). It was found that the flow was dominated by the collision of the boundary layers in the region between the hot and the cold surfaces.

Previously, colliding boundary layer situation has received very little attention with numerical analysis reported by Kubleck *et al.* (1980) and de Vahl Davis (1989) both for laminar and Turbulent flow conditions. Recent studies by Gatheri and Sigey (1999) who both investigated in detail turbulence flow in a three dimensional enclosure in the form of a room

containing a conventional heater built into one wall having a window in the same wall. The size of the window was varied to pave way for two cases of study but center fixed with respect to the heater. The results of the study indicated that the rate of heat transfer is higher for a larger window than for a small window as the Raylegh number increases.

From the above discussion it follows that the numerical simulation of laminar flow in a room with a window and a heater is yet to be done. It is for this reason that this project seeks a systematic study of a three dimensional enclosed cavity in form of a room which is differentially heated on one wall and cooled on the same wall.

1.3 Aim of the project

The main objective of this study is to investigate the colliding boundary layer as a result of localized heating and cooling on the same wall caused by non-uniformity of the boundary temperature. Non-uniform thermal boundary conditions are encountered in many engineering and domestic applications e .g building walls are rarely isothermal and more often than not they have hot and cold regions.

The scope of the study is limited to three-dimensional steady-state laminar free convection in a rectangular enclosure and predictions are made within

the framework of finite difference method in numerical technique. A computer code capable of simulating this is required in order to realize the aim of this work . A simple geometrically enclosure is chosen with a window and a heater mounted below it.

1.4 Project outline

In Chapter 1 effort has been made in outlining various researchers who have preceded this work using various methodologies i.e. experimental, analytical, and. numerical for both two and three dimensional cases.

In Chapter two, a complete set of equations governing the motion of a Newtonian fluid were presented.in general form , since these equations are necessary in the analysis of fluid flow problems. Being in general form, they can be used to solve most fluid flow problems.

They are then non-dimensinalised and the primitive variables notably the pressure and problem of solving continuity equation is overcome by recasting the momentum equation in a vorticity-vector potential formulation (Mallison and de Vahl Davis 1977).

In Chapter three, a particular problem of three-dimensional laminar natural convection in a rectangular cavity with boundary that defines it, is posed. Governing equations presented in the previous chapter are then simplified by

use of Boussinesq approximation resulting in a set of simplified conservation equations.

In Chapter four the numerical method used to solve the finite difference equations is presented. The conservation equations together with the boundary conditions are discretized using a three- point central difference approximation for non-uniform mesh. The resulting finite difference equations were then solved using the method of false transients and the Samarskii-Andreyev scheme. The method of solution for the overall solution procedure is outlined in this chapter.

The results of a computer program which involved the conservative equations and the various constants and variables earlier discussed are presented in chapter five. Being in form of graphs, the results are discussed in the same chapter. Conclusions and recommendations is given in Chapter six.

CHAPTER TWO

Mathematical formulation

Equations governing free convection

2.1 Introduction

In free convection, fluid motion is due to buoyancy forces within the fluid. Buoyancy is due to the combined presence of a fluid density gradient and a body force that is proportional to density. In practice the body force is gravitational.

An essential step in the treatment of any convection problem is to determine whether the boundary conditions are laminar or turbulent because surface friction and the convective transfer rates depend strongly on which of these conditions exists.

Naturally occurring flows are either turbulent or laminar. In laminar flow, motion is highly ordered and it is possible to identify streamlines along which particles move. In turbulent flow however, the parameters such as velocity, pressure and temperature at any given time vary rapidly and randomly with time. In either case, the flow starts with laminar then turbulent.

In this chapter, we consider the equations governing the behavior of Newtonian fluid experiencing heat or mass transfer. These equations

originate from the conservation principles. The specific processes such as the inertia and the viscous forces remain important, as does the energy transfer by advection and diffution. Considering a fluid in which the density ρ is a function of position x_j (j =1,2,3). Let u_j (j =1,2,3) denote the components of the velocity. Hence in writing the various equations, use of the notation of Cartesian tensors with the usual summation convection is applied. Derivation of these equations is found in most of the fluid mechanics books, in particular reference. to; Batchalor (1954),Aris (1962), Currie (1974) and Anderson (1984).

Leonardi (1984) presented a unique derivation of these equations in their most general form. The governing equations are the continuity, momentum and energy equation.

2.2 **Conservation Equations**

2.2.1The continuity equation

The law of conservation of mass states that the rate of increase of mass within a controlled volume is equal to the net rate of influx through the control surface. Thus the continuity equation can be written as

$$\frac{\partial \rho}{\partial t} + \frac{\partial}{\partial x_j}(\rho \mu_i) = 0 \qquad (2.1)$$

For steady state however, equation (2.1) becomes

$$\frac{\partial}{\partial x_j}(\rho \mu_i) = 0 \qquad (2.2)$$

2.2.2 **Momentum equation**

This is derived from the Newton second law of motion. It states that the sum of the body and surface forces acting on a system is equal to the time rate of change of linear momentum of the system. Given that the only force considered in this work is only the gravitational force then $f_i=g_i$ in the x-direction. Thus the equation become:

$$\rho F_i + \frac{\partial}{\partial x_j}(\Pi_{ij}) = \frac{\partial}{\partial t}(\rho \mu_i) + \frac{\partial}{\partial x_i}(\mu_i \mu_j) \qquad (2.3)$$

Where

ρF_i = Body force per unit volume

Π_{ij} = stress tensor.

Note that for Newtonian fluids,

$\Pi_{ij} = -p\delta_{ij} + \tau_{ij}$ (White 1974) (2.4)

Where,

δ_{ij} = Kronecker delta with values of1 for $i = j$ and 0 for $j \neq i$

τ_{ij} = Viscous stress tensor

and,

Φ is the viscous dissipation function given by,

$$\Theta = T_{ij}\frac{\partial u_i}{\partial x_j} \tag{2.9}$$

h is the specific enthalpy and

q_j is the local rate of. heat transfer per unit area.

In this case heat produced by external forces is neglected

The heat transfer is modelled by Fourier's law viz

$$q_j = -\lambda\frac{\partial T}{\partial x_j}$$

Where λ is the thermal conductivity.

Given h can be defined as,

$$h = e + \frac{p}{\rho} \tag{2.11}$$

Where e is the specific internal energy, equation (2.8) can hence be simplified .The differential form of equation (2.11) becomes

$$dh = de + \frac{\partial p}{\rho} + pd\left(\frac{1}{\rho}\right) \tag{2.12}$$

It is possible however to write

$$\tau_{ij} = \mu\left(\frac{\partial \mu_i}{\partial x_j} + \frac{\partial \mu_j}{\partial x_i}\right) + \mu_s \delta_{ij} \frac{\partial \mu_k}{\partial x_k} \tag{2.5}$$

Where μ and μ_s are the first and second coefficient of viscosity respectively. Thus it follows,

$$\Pi_{ij} = -p\delta_{ij} + \mu\left(\frac{\partial \mu_i}{\partial x_j} + \frac{\partial \mu_j}{\partial x_i}\right) + \mu_s \delta_{ij} \frac{\partial \mu_k}{\partial x_k} \tag{2.6}$$

Noting that the only type of force being considered in this project is the gravitational then,

$F_i = g_i$

Thus on substituting equation (2.6) in (2.3) the equation become:

$$\frac{\partial}{\partial t}(\rho \mu_i) + \frac{\partial}{\partial x_j}(\rho \mu_i \mu_j) = -\frac{\partial \rho}{\partial x_j} + \rho g_i + \frac{\partial}{\partial x_j}\left[\mu\left(\frac{\partial u_i}{\partial x_j} + \frac{\partial u_j}{\partial u_i}\right) + \mu_s \delta_{ij} \frac{\partial u_k}{\partial x_k}\right] \tag{2.7}$$

2.2.3 The energy equation

This is derived from the first law of thermodynamics, which states that the rate of energy increase in a system is equal to the heat added to the system and the work done on the system. Assuming no external heat sources, the energy equation is often written as (Currie (1974)).

$$\rho \frac{\rho h}{\partial t} + \frac{\partial p}{\partial x_j}(\rho u_j h) = \frac{\partial p}{\partial t} + \frac{\partial}{\partial x_j}(u_j p) - \frac{\partial q_i}{\partial x_j} + \Phi \tag{2.8}$$

Where,

$$de = Tds - pd\frac{1}{\rho} \tag{2.13}$$

Where S is the entropy, using the first and second law of thermodynamics (Hatsopoulous and Keenan (1965)).

When the above equation is substituted in (2.12) the differential of specific enthalpy (h) becomes

$$dh = TdS + dp\left(\frac{1}{\rho}\right) \tag{2.14}$$

Given that the entropy depends on temperature and pressure, then it can be written as,

S=S (T, P)

Such that,

$$dS = \left(\frac{\partial S}{\partial p}\right)_T dp + \left(\frac{\partial s}{\partial T}\right)_P dT$$

Since for free convection effects; highly depend on the volumetric coefficient (β) then using the general thermodynamics relations (Hatsopoulous and Keenan 1965).

$$\left(\frac{\partial S}{\partial P}\right)_T dP = \frac{\beta}{\rho}\left(\frac{\partial S}{\partial T}\right)_p dT = \frac{C_P}{T}$$

$$\left(\frac{\partial S}{\partial p}\right)_T dP = -\frac{\beta}{\rho}, \left(\frac{\partial S}{\partial T}\right)_P dT = -\frac{\beta}{\rho}$$

$$\left[\frac{\partial \frac{1}{\rho}}{\partial T}\right]_P = -\frac{\beta}{\rho}$$

Substituting the above in equation (2.15) results in

$$dS = -\frac{\beta}{\rho}dP + \frac{C_p}{T}dT \qquad (2.6)$$

Where C_p is the specific heat at constant pressure.

Substituting (2.16) into (2.14) results in:

$$dh = c_p dT + \frac{1}{\rho}(1-\beta T)dP \qquad (2.17)$$

When (2.17) and (2.10) are substituted in (2.8) the final form of the energy equation is written as

$$\frac{\partial}{\partial t}(\rho c_p T) + \frac{\partial}{\partial x_j}(\rho u_j T) = \frac{\partial}{\partial x_J}\left(\lambda \frac{\partial T}{\partial x_j}\right) + \beta T\left(\frac{\partial p}{\partial t} + \frac{\partial u_j p}{\partial x_j}\right) + \Phi \qquad (2.18)$$

The above equations (2.1), (2.7) and (2.18) for the continuity, mean momentum and mean energy respectively are however in their most general form, hence appropriate boundary conditions together with the equations are necessary for determining the velocity component u and the fluid properties such as density ρ pressure P and temperature T which apply to laminar flow. It is worthy noting that numerical approach has proved to be efficient in solving the above conservation equations rather than the exact methods.

2.3 Non- dimensionalisation

Non-dimensionalisation of variables is an automatic procedure for numerical as well as experimental studies of fluid flow. Thus an adoption of a suitable non-dimensional scheme is very important. In doing this, the solution obtained is generalized and the variables are bounded e.g temperature can be non-dimentionalised so that its values vary between 0 and 1. The main rationale in non-dimentionalisation is to reduce the number of parameters particularly when dealing with incompressible fluids.

This is because in compressible fluids the number of non-dimensional parameters is equivalent to the dimensional parameters Leonardi *et al.* (1981), hence such reasoning becomes invalid However the assumption made in this work is that the fluid is incompressible. To non-dimentionalise the above equations therefore all lengths are divided by the characteristic length L_R, all velocities are divided by arbitrary reference velocity and pressure by arbitrary reference pressure.

The non-dimentionalisation is performed using the following scaling variable:

$$X_j = X_j' L_R \qquad P = P' P_R$$

$$U_j = U_j U_*$$

$$\Theta = \frac{T - T_*}{T_H - T_C}$$

$$\rho = \rho' \rho_R$$

$$\mu_s = \mu'_s \mu_R$$

$$P = P' P_R$$

$$V = V' U_R$$

$$c_p = c_p c_{pR}$$

$$\lambda = \lambda' \lambda_R$$

$$t = \frac{t' \lambda_R}{U_*}$$

Where L_R is the characteristic length; T_H-T_C is the characteristic temperature difference and T_* is a convenient temperature which will result in the Non-dimensional mean temperature (Θ) being bounded in the solution region. In the above scaling variables the primes denote non-dimensional quantities and the subscripts $*$ denote variables that can be arbitrarily defined to specify a non-dimensional scheme.

The application of the above scaling variable to the continuity equation (2.1), the mean momentum equation (2.7) and the mean energy equation (2.18) result in

$$\frac{\partial \rho'}{\partial t} + \frac{\partial}{\partial x_j'} \rho' u_j' = 0 \tag{2.19}$$

$$\frac{\partial}{\partial t'} \rho' \mu_i' + \frac{\partial}{\partial x_j'} \rho' \mu_i' \mu_j' = -\left\{\frac{P_R}{\rho_R U_*^2}\right\} \frac{\partial P'}{\partial x_j'} + \left\{\frac{g L_R}{U_*^2}\right\} \rho g_i' + \frac{\partial}{\partial x_j} \left\{\frac{\mu_R}{\rho_R U_* L_R}\right\} \tau_{ij} \tag{2.20}$$

$$\frac{\partial}{\partial t'}\left(c_p' \rho' \Theta\right) + \frac{\partial}{\partial x_j'} c_p' \rho' u_j' \Theta = \left\{\frac{P_R}{c_{PR} \rho_R \Delta T_*}\right\} \left(\frac{\partial P'}{\partial t'} + u_j' \frac{\partial p'}{\partial x_j}\right) + \frac{\partial}{\partial x_j}\left(\left\{\frac{\lambda_R}{c_{PR} \rho_R U_* L_R}\right\}\right)\left\{\frac{\mu_R U_*}{c_{RP} \rho_R \Delta}\right\}$$

$$\lambda \frac{\partial \Theta}{\partial x_j} + \left\{\frac{\mu_R U_*}{c_{PR} \rho_R \Delta_* L_R}\right\} \Phi \tag{2.21}$$

The results in the variable hence become non-dimensional and of unit magnitude (de Vahl Davis 1986). A tendency of thin boundary layers do form on the cavity walls and viscous effects are confined to these thin regions if the temperature difference across the cavity is large and viscocity of fluid is small over most of the cavity. In such a case, solely buoyancy forces will balance viscous effects. An appropriate scheme is introduced in which the characteristic velocity is

$$U^* = \sqrt{g \beta \Delta T_* L_R} \tag{2.22}$$

The scale factor for the above scheme has focused attention on the momentum equation. Similarly from energy equation in steady state, the convection and conduction terms must balance, hence appropriate to introduce a scheme in which the coefficient of the two terms are the same. Thus,

$$U^* = \frac{\lambda_R}{\rho_R c_P L_R} \tag{2.23}$$

The above two schemes have been applied in solving many natural convection problems by researchers like de Vahl Davis (1986), Leonardi (1984), Henkes (1990), Lankhorst (1991).

Hereafter all variables and equations are assumed to be non-dimensional so that without ambiquity the primes have been omitted. Since a number of non-dimensional schemes are possible equations 2 9 to 2.11 are written in general form viz

$$\frac{\partial \rho}{\partial t} + \frac{\partial}{\partial x_j} \rho u_j = 0 \tag{2.24}$$

$$\frac{\partial}{\partial t}\rho u_i + \frac{\partial}{\partial x_j}\rho u_i u_j = -E_1\frac{\partial p}{\partial x_i} + E_2\rho g_i + \frac{\partial}{\partial x_j}E_3\tau_{ij} \tag{2.25}$$

$$\frac{\partial}{\partial t}c_P\rho\Theta + \frac{\partial}{\partial x_j}c_P\rho u_j\Theta = C_1\left(\frac{\partial P}{\partial t} + u_j\frac{\partial P}{\partial x_j}\right) + \frac{\partial}{\partial x_j}\left(C_2\lambda\frac{\partial\Theta}{\partial x_j}\right) + C_3\Phi \tag{2.26}$$

Where the coefficient E_1, E2 ,E_3 ,C_1 ,C_2 and C_3 are given as,

$$E_1 = \frac{P_R}{\rho_R} \qquad E_2 = \frac{g\,L_R}{U_*^2}$$

$$E_3 = \frac{\mu_R}{\rho_R U_* L_R} \qquad C_1 = \frac{P_R}{\rho_R c_{PR}\Delta T_*}$$

$$C_2 = \frac{\lambda_R}{C_{PR}\rho_R\Delta T_* L_R} \qquad C_3 = \frac{\mu_R U_*}{C_{PR}\rho_R\Delta T_* L_R}$$

The set of equations presented in this chapter contain more unknowns than the number of equations present, this is not possible to solve. In the preceding chapter the cross term correlation in the mean equations are modeled in terms of quantity that are known or which can be calculated.

CHAPTER THREE

1.0 Mathematical model

The equations presented in chapter two are general and are applicable to most fluid flow situations. In this chapter a specific model will be presented.

3.1 Geometry of model

The model to be studied in the determination of the flow and thermal fluid is a three dimensional rectangular cavity illustrated in Figure 3.1 as shown below. A brief look at the literature survey reveals that there is no standard definition of characteristic length for such a case, although the most common dimension chosen as the characteristic length is L_R, which is taken as the size of the enclosure in the z-direction. Various numerical computations have been carried out for the model with boundary conditions simulating a heated room. The enclosure is heated by a conventional heater (H) that is mounted below a window on one of the walls generally referred as 'active wall', as illustrated in the figure.

All the boundaries of the enclosure are assumed to be non-slip, rigid and impermeable. That is there is no through flow and so the mass of the fluid within the cavity is constant. Each of the remaining walls of the enclosure may be adiabatic, isothermal, or have a specific heat flux through it.

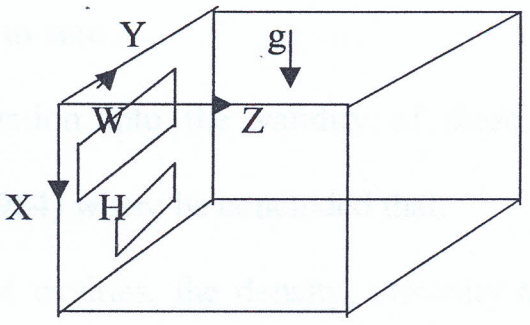

Figure 3.1 The geometrical model with co-ordinates system.

3.2 Boussinesq Approximation

In deriving the equations in the preceding section the only assumption made was that the fluid is Newtonian, steady and that there are no internal heat sources within the model. However, as pointed out by Boussinesq (1903) there are many situations of practical occurrence in which the basic equations can be simplified considerably. These situations occur when the variability in the density and in the various coefficients is due to variation of temperature of only moderate amounts.

It is thus for this reason that the Boussinesq approximation will be applied, and the assumption associated with this simplification are that:

1: All fluid properties, except the density, are assumed constant.

2: Density variations are only significant when buoyancy forces cause it, and it varies linearly with temperature.

3: The viscous dissipation effects may be neglected.

4: The characteristic temperature difference (T_H-T_C) be sufficiently small that it tends to zero

An investigation into the validity of these assumptions was made by Leonardi (1984) where he concluded that:

"In air filled cavities, the density, viscosity and conductivity must all be variable if the temperature difference within the region of interest is above 30K . In water filled cavities, density and viscosity must be variable if the temperature difference is above 3K". The application of this assumption allows the buoyant forces to be well handled. The coefficients β, v and ρ_r are treated as constants and evaluated at a reference temperature T_R

Given density varies linearly with temperature only, it follows that:

$$\rho = \rho_R + (T - T_R)\left(\frac{\partial \rho}{\partial T}\right)_{T_R} \tag{3.1.}$$

In which the higher order terms of this series have been neglected. The coefficient of thermal expansion at constant pressure is defined as

$$\beta_R = -\frac{1}{\rho_R}\left(\frac{\partial P}{\partial T}\right)_{T_{R_R}} \tag{3.2}$$

on substituting, yields

$$\rho = \rho_R(1 - \beta_R(T - T_R)) \tag{3.3}$$

Now applying the Boussinesq approximation and the use of the above equation into momentum equation, the equation governing natural convection within the cavity are presented in non-dimensional form for an incompressible laminar flow as:

$$\frac{\partial u_j}{\partial x_j} = 0 \tag{3.4}$$

$$\frac{\partial u_i u_j}{\partial x_j} = -\frac{E_1}{\rho_R}\frac{\partial P}{\partial x_i} - E_2 \Theta g_i + \frac{\partial}{\partial x_j} E_3 \left(\frac{\partial u_i}{\partial x_j} + \frac{\partial u_j}{\partial x_i} \right) \tag{3.5}$$

$$\frac{\partial \Theta}{\partial t} + \frac{\partial}{\partial x_j} u_j \Theta = \frac{\partial}{\partial x_j} C_2 \frac{\partial \Theta}{\partial x_j} \tag{3.6}$$

In the momentum equation,(3.6) the coefficient $E_2 = (E_2)_{old} \beta_R \Delta T_*$ where $(E_2)_{old}$ is given in section 2.3

The density terms, which have not been neglected in the above equations, do generated motion.

Note that the equations above are in conservative form and to achieve more accurate results is when they are implemented in finite difference form.

3.3 The vorticity/vector potential formulation

The governing equations mentioned earlier on can be solved in a variety of ways. The most obvious way is to solve the conservation equations in the primitive variable form. However the main drawbacks of this method and which makes it unpopular to many researchers is that the conservation of mass

is not guaranteed. Similarly the accurate implementation of boundary condition for pressure has shown to be difficulty. Phillip and Schmidt (1984). As a result of these drawbacks associated with this formulation, other ways had to be devised. One such way is the Vorticity/Velocity formulation. In this method, the troublesome pressure is eliminated by taking the curl of the momentum equation, which inturn yields the vorticity transport equation.

Stella *et al.* (1988) showed that this formulation gives accurate results only when a uniform staggered mesh has been chosen, thus for non-uniform mesh points the formulation proved to be ineffective.

A method that enforces continuity and eliminates the pressure term from the momentum Equation is the Vorticity Vector potential formulation

3.3.2 The Vorticity Transport Equation

For a two-dimensional flow, the non-dimensional continuity equation and the momentum equation can be written in expanded Cartesian co-ordinate system as

$$\frac{\partial u}{\partial u}+\frac{\partial v}{\partial y}=0 \qquad \textbf{(3.7)}$$

$$\frac{\partial u}{\partial t}+u\frac{\partial u}{\partial x}+v\frac{\partial u}{\partial y}=\frac{E_1}{\rho_R}\frac{\partial P}{\partial x}-E_2\Theta COS\gamma+\frac{\partial}{\partial x}\left[(E_3+V)2\frac{\partial U}{\partial x}-\frac{2}{3}v\right]+\frac{\partial}{\partial y}\left[(E_3+\nu)\frac{\partial u}{\partial y}+\frac{\partial v}{\partial x}\right] \qquad \textbf{(3.8)}$$

$$\frac{\partial v}{\partial t}+u\frac{\partial v}{\partial x}+v\frac{\partial v}{\partial y}=-\frac{E_1}{\rho_R}\frac{\partial P}{\partial y}-E_2\Theta SIN\gamma+\frac{\partial}{\partial x}\left[(E_3+v)\left(\frac{\partial v}{\partial x}+\frac{\partial u}{\partial y}\right)\right]+\frac{\partial}{\partial y}\left[(E_3+v)2\left(\frac{\partial v}{\partial y}\right)-\frac{2}{3}v\right]$$

(3.9)

where γ is the angle between the gravitational vector and x-axis.

The problem of obtaining a solution that satisfies the continuity for two-dimensional is overcome by introduction of the stream function Ψdefined

$$u=\frac{\partial \Psi}{\partial y}, v=-\frac{\partial \Psi}{\partial x}$$

$\Psi(x,y)$ automatically satisfied the continuity equation since the vorticity ζ is defined as

$$\zeta=\frac{\partial v}{\partial x}-\frac{\partial u}{\partial y} \qquad (3.10)$$

Substituting yields

$$\frac{\partial^2 \Psi}{\partial x^2}+\frac{\partial^2 \Psi}{\partial y^2}=-\zeta \qquad (3.11)$$

Taking the curl of the momentum equation eliminates the pressure as a solution variable and yields the vorticity transport equation.

$$\frac{D\zeta}{Dt}=(E_3+v)\nabla^2\zeta+2\left(\frac{\partial v}{\partial x}\frac{\partial \zeta}{\partial x}+\frac{\partial v}{\partial y}\frac{\partial \zeta}{\partial y}\right)-(\nabla^2 v)\zeta+2\left(\frac{\partial^2 v}{\partial x^2}\frac{\partial v}{\partial x}-\frac{\partial^2 v}{\partial y^2}\frac{\partial u}{\partial y}+2\frac{\partial^2 v}{\partial x\partial y}\frac{\partial v}{\partial y}\right)$$

$$-E_2\left(\frac{\partial \Theta}{\partial x}\sin\gamma-\frac{\partial \Theta}{\partial y}\cos\gamma\right) \qquad (3.12)$$

The above equation has replaced the primitive variable equation (3.7) and (3.8) as long as the boundary conditions for the stream function and vorticity are consistent with those of the velocity.

The main advantage of this method is that, the continuity equation is automatically satisfied, it does not require a staggering finite difference grid system and the number of equations to be solved are reduced (de Vahl Davis 1983).

However this method worked very well for two-dimensional convection problems.

3.3.2 The vorticity vector potential formulation

This approach has not be used for complicated cases of three dimensional convection flow due to a number of reasons:-

-the number of differential equations to be solved is not reduced in cases of three dimensional flows.

-there is lack of understanding of its boundary conditions.

As results, existing implementations have been restricted to the simplest cases, where the solution region is closed and simply connected.

The vector potential ψ is defined by $u = \nabla \times \psi$ and is assumed to be solenoidal $(\nabla \cdot \psi = 0)$ the vector potential is related to vorticity by

$$\zeta = -\nabla^2 \psi \qquad (3.13)$$

By recasting the momentum equation in a vorticity vector potential, the problem associated with the use of primitive variables, the pressure and the requirement of solving the continuity equation is overcome (Mallinson and de Vahl Davis (1977)).

By taking the curl of the momentum equation (3.8) the vorticity transport equation results (Ozoe et al.1976)

$$\frac{\partial \zeta_1}{\partial t}+u\frac{\partial \zeta_1}{\partial x}+V\frac{\partial \zeta_1}{\partial z}-\zeta_2\frac{\partial u}{\partial y}-\zeta_3\frac{\partial u}{\partial z}=(E_3+V)\nabla^2\zeta_1+\frac{\partial V}{\partial x}\frac{\partial \zeta_1}{\partial x}+2\frac{\partial V}{\partial y}\frac{\partial \zeta_2}{\partial y}+2\frac{\partial V}{\partial z}\frac{\partial \zeta_1}{\partial z}$$

$$-\frac{\partial V}{\partial y}\frac{\partial \zeta_2}{\partial x}-\frac{\partial V}{\partial z}\frac{\partial \zeta_3}{\partial x}-\left(\frac{\partial^2 V}{\partial y^2}+\frac{\partial^2 V}{\partial z^2}\right)\zeta_1+\frac{\partial^2 V}{\partial x\partial y}\zeta_2+\frac{\partial^2 V}{\partial x\partial z}$$

$$+\left[\frac{\partial^2 V}{\partial x\partial y}\frac{\partial w}{\partial x}+\frac{\partial^2 V}{\partial y^2}\frac{\partial w}{\partial y}+\frac{\partial^2 V}{\partial y\partial z}\frac{\partial w}{\partial z}-\left(\frac{\partial^2 V}{\partial x\partial z}\frac{\partial v}{\partial x}+\frac{\partial^2 V}{\partial y\partial z}\frac{\partial v}{\partial y}+\frac{\partial^2 V}{\partial z^2}\frac{\partial v}{\partial z}\right)\right] \qquad (3.14)$$

similarly

$$\frac{\partial \zeta_2}{\partial t}+u\frac{\partial \zeta_2}{\partial x}+v\frac{\partial \zeta_2}{\partial y}+w\frac{\partial \zeta_2}{\partial z}-\zeta_1\frac{\partial v}{\partial x}-\zeta_2\frac{\partial v}{\partial y}-\zeta_3\frac{\partial v}{\partial z}=(E_3+V)\nabla^2\zeta_2$$

$$+2\left[\frac{\partial V}{\partial x}\frac{\partial \zeta_2}{\partial x}+\frac{\partial V}{\partial y}\frac{\partial \zeta_2}{\partial y}\right]+2\left[\frac{\partial V}{\partial z}\frac{\partial \zeta_2}{\partial z}-\frac{\partial V}{\partial x}\frac{\partial \zeta_1}{\partial y}-\frac{\partial V}{\partial z}\frac{\partial \zeta_1}{\partial y}\right]-\zeta_2\left[\frac{\partial^2 V}{\partial x^2}+\frac{\partial^2 V}{\partial z^2}\right]$$

$$\frac{\partial^2 V}{\partial x\partial y}\zeta_1+\frac{\partial^2 V}{\partial y\partial z}\zeta_3-E_3^2\frac{\partial \Theta}{\partial z}+2\left[\frac{\partial^2 V}{\partial x\partial z}\frac{\partial u}{\partial x}+\frac{\partial^2 V}{\partial y\partial z}\frac{\partial u}{\partial y}+\frac{\partial^2 V}{\partial z\partial y}\frac{\partial u}{\partial z}-\left(\frac{\partial^2 V}{\partial x^2}\frac{\partial w}{\partial x}+\frac{\partial^2 V}{\partial x\partial y}\frac{\partial w}{\partial y}+\frac{\partial^2 V}{\partial x\partial z}\frac{\partial w}{\partial z}\right)\right] \qquad (3.15)$$

finally,

$$\frac{\partial \zeta_3}{\partial t}+u\frac{\partial \zeta_3}{\partial x}+v\frac{\partial \zeta_3}{\partial y}+w\frac{\partial \zeta_3}{\partial z}-\zeta_1\frac{\partial w}{\partial y}-\zeta_3\frac{\partial w}{\partial z}-\zeta_3\frac{\partial v}{\partial z}=(E_3+V)\nabla^2\zeta_3$$

$$+2\left[\frac{\partial V}{\partial x}\frac{\partial \zeta_3}{\partial x}+\frac{\partial V}{\partial y}\frac{\partial \zeta_3}{\partial y}\right]+\frac{\partial V}{\partial z}\frac{\partial \zeta_3}{\partial z}-\frac{\partial V}{\partial x}\frac{\partial \zeta_1}{\partial z}-\frac{\partial V}{\partial y}\frac{\partial \zeta_2}{\partial z}-\left[\frac{\partial^2 V}{\partial x^2}+\frac{\partial^2 V}{\partial y^2}+\frac{\partial^2 V}{\partial x\partial z}\zeta_1+\frac{\partial^2 V}{\partial y\partial z}\zeta_2+E_2\frac{\partial}{\partial}\right.$$

$$+2\left[\frac{\partial^2 V}{\partial x^2}\frac{\partial v}{\partial x}+\frac{\partial^2 V}{\partial x\partial y}\frac{\partial v}{\partial y}+\frac{\partial^2 V}{\partial x\partial z}\frac{\partial v}{\partial z}-\left(\frac{\partial^2 V}{\partial x\partial x}\frac{\partial u}{\partial x}+\frac{\partial^2 V}{\partial y^2}\frac{\partial u}{\partial y}+\frac{\partial^2 V}{\partial y\partial z}\frac{\partial u}{\partial z}\right)\right] \qquad (3.16)$$

The above equations (3.14), (3.15), (3.16) may therefore replace the momentum and the continuity equations.

3.4 Boundary conditions

To complete the mathematical formulation, boundary conditions for all the variables are necessary.

3.4.1 Temperature boundary condition.

Thermal boundary layer occurs when the fluid flow stream and surface temperatures differ

The non-dimensional temperature has earlier been defined as

$$\Theta=\frac{T-T_*}{T_H-T_C} \qquad (3.17)$$

Where

T_H is the temperature of a hot wall and

T_C is the temperature of a cold wall.

With the above definition the value of Θ is bounded and lies between 0 and 1. The three thermal boundary conditions commonly implemented are the isothermal, adiabatic, and convective boundary conditions which may be represented by the equation

$$A_1 + \frac{\partial \Theta}{\partial n} + A_2 \Theta + A_3 = 0 \qquad (3.18)$$

Where

n refers to the direction normal to the wall.

Θ = Constant

The boundary condition is thus isothermal if A_1=0 and Θ = Constant

The boundary condition is said to be adiabatic if $A_2 = A_3 = 0$

Whilst non-zero A_1 and $A_2 = 0$ represents a convective heat flux boundary condition. Since the problem at hand involves heating and cooling on the same wall, then the remaining walls of the enclosure are kept either adiabatic, isothermal or have a specified heat flux through them.

3.4.2 Velocity boundary conditions

The conditions in the motion of the fluid at a boundary are mostly specified in terms of the velocity. Velocity boundary layer develops whenever there is fluid flow over a surface .In closed enclosures each boundary is considered impermeable and capable only of motion in its place (static motion). This

implies that the normal component of velocity at each boundary is zero .e .g considering the boundary x=0. The impermeable condition implies that u = 0 if the plane is stationary.

Similarly

$$v = w = 0 \tag{3.19}$$

3.4.3 vector potential boundary condition

These boundary conditions were first proposed by Hirasaki and Hellums (1968) and were later modified and implemented by Mallison *et al.* (1973).

The boundary condition for the vector potential ensures that the velocity field satisfies the conditions of impermeable boundary. Hirasaki and Hellums (1968) introduced a scalar potential to account for through-flow But since the walls in the model of interest are assumed to be impermeable. then the scalar potential becomes non existent.

They further showed that for a region with no through flow, the appropriate boundary conditions are:

$$\psi_{t1} = \psi_{t2} = \frac{\partial \psi_n}{\partial n} = 0 \tag{3.20}$$

where

$\psi_{t1} = \psi_{t2}$ are tangential components of the vector potential at the boundary and:

$\frac{\partial \psi_n}{\partial n}$ is the normal derivative of the normal component.

3.4.4 Vorticity boundary condition

As outlined by Mallison and de Vahl Davis (1977) the vorticity boundary conditions are obtained from equation (3.4)

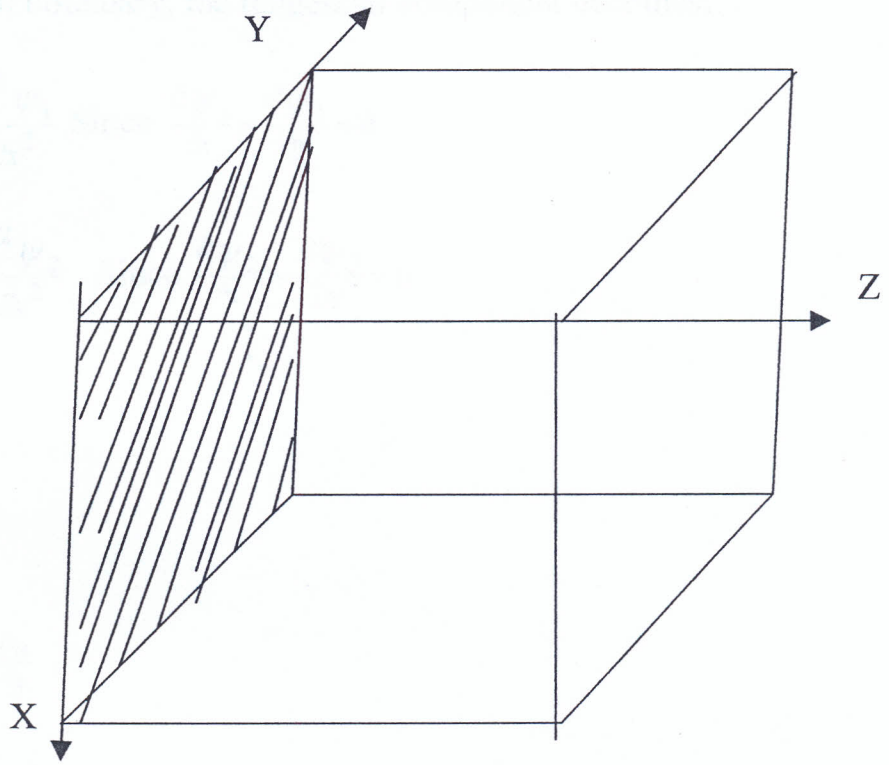

Figure 3.2 illustration of vorticity boundary condition on the wall z=0.

$$-\zeta = \frac{\partial^2 \psi}{\partial x^2} + \frac{\partial^2 \psi}{\partial y^2} \qquad (3.21)$$

Consider the shaded wall z=o in the above figure, then equation (3.21) may be written as

$$-\zeta_1 = \frac{\partial^2 \psi_1}{\partial x^2} + \frac{\partial^2 \psi_1}{\partial y^2} + \frac{\partial^2 \psi_1}{\partial z^2}$$

$$-\zeta_2 = \frac{\partial^2 \psi_2}{\partial x^2} + \frac{\partial^2 \psi_2}{\partial y^2} + \frac{\partial^2 \psi_2}{\partial z^2}$$

$$-\zeta_3 = \frac{\partial^2 \psi_3}{\partial x^2} + \frac{\partial^2 \psi_3}{\partial y^2} + \frac{\partial^2 \psi_3}{\partial z^2}$$

At the z=0 boundary, the tangential component becomes:

$$-\zeta_1 = -\frac{\partial^2 \psi_1}{\partial x^2} \quad \text{Since } \frac{\partial \psi_1}{\partial x} = \frac{\partial \psi_1}{\partial y} = 0 \tag{3.22}$$

$$-\zeta_2 = -\frac{\partial^2 \psi_2}{\partial x^2} \quad \text{Since } \frac{\partial \psi_2}{\partial x} = \frac{\partial \psi_2}{\partial y} = 0 \tag{3.23}$$

But

$$\zeta = \nabla \times v$$

Hence

$$\zeta_3 = \frac{\partial v}{\partial x} - \frac{\partial u}{\partial y}$$

since,

$$\frac{\partial v}{\partial x} = \frac{\partial u}{\partial y} = 0 \qquad \text{at z=0}$$

Similar procedure may be used to derive for the other walls,i.e at x=0 and at y=0.

3.5 Partial Differential Equations In Component Form

3.5.1 Vorticity Transport Equations

$$\frac{V_3}{\alpha_\zeta}\frac{\partial \zeta_1}{\partial t} = -V_1\frac{\partial}{\partial Y}(\zeta_1 V) - V_1\frac{\partial}{\partial Z}(\zeta_2 W) + V_1\frac{\partial}{\partial Y}(\zeta_2 U) + V_1\frac{\partial}{\partial Z}(\zeta_3 U)$$

$$-V_2\frac{\partial}{\partial Y}(\theta g_3) + V_2\frac{\partial}{\partial Z}(\theta g_2)$$

$$+V_3\frac{\partial^2 \zeta_1}{\partial X^2} + V_3\frac{\partial^2 \zeta_1}{\partial Y^2} + V_3\frac{\partial^2 \zeta_1}{\partial Z^2} \qquad (3.24)$$

$$\frac{V_3}{\alpha_\zeta}\frac{\partial \zeta_2}{\partial t} = -V_1\frac{\partial}{\partial Z}(\zeta_2 W) - V_1\frac{\partial}{\partial X}(\zeta_2 U) + V_1\frac{\partial}{\partial X}(\zeta_1 V) + V_1\frac{\partial}{\partial Z}(\zeta_3 V)$$

$$-V_2\frac{\partial}{\partial Z}(\theta g_1) + V_2\frac{\partial}{\partial X}(\theta g_3)$$

$$+V_3\frac{\partial^2 \zeta_2}{\partial X^2} + V_3\frac{\partial^2 \zeta_2}{\partial Y^2} + V_3\frac{\partial^2 \zeta_2}{\partial Z^2} \qquad (3.25)$$

$$\frac{V_3}{\alpha_\zeta}\frac{\partial \zeta_3}{\partial t} = -V_1\frac{\partial}{\partial X}(\zeta_3 U) - V_1\frac{\partial}{\partial Y}(\zeta_3 V) + V_1\frac{\partial}{\partial X}(\zeta_1 W) + V_1\frac{\partial}{\partial Z}(\zeta_2 W)$$

$$-V_2\frac{\partial}{\partial X}(\theta g_2) + V_2\frac{\partial}{\partial Y}(\theta g_1)$$

$$+V_3\frac{\partial^2 \zeta_3}{\partial X^2} + V_3\frac{\partial^2 \zeta_3}{\partial Y^2} + V_3\frac{\partial^2 \zeta_3}{\partial Z^2} \qquad (3.26)$$

3.5.2 Energy equation

$$\frac{E_2}{\alpha_\theta}\frac{\partial\theta}{\partial t} = -E_1\frac{\partial}{\partial X}(\theta U) - E_1\frac{\partial}{\partial Y}(\theta V) - E_1\frac{\partial}{\partial Z}(\theta W)$$

$$+E_2\frac{\partial^2\zeta}{\partial X^2} + E_2\frac{\partial^2\zeta}{\partial Y^2} + E_2\frac{\partial^2\zeta}{\partial Z^2} \tag{3.27}$$

3.5.4 Velocity-Vector potential

$$\frac{1}{\alpha_\psi}\frac{\partial\psi_1}{\partial t} = \zeta_1 + \frac{\partial^2\psi_1}{\partial x^2} + \frac{\partial^2\psi_1}{\partial y^2} + \frac{\partial^2\psi_1}{\partial z^2} \tag{3.28}$$

$$\frac{1}{\alpha_\psi}\frac{\partial\psi_2}{\partial t} = \zeta_2 + \frac{\partial^2\psi_2}{\partial x^2} + \frac{\partial^2\psi_2}{\partial y^2} + \frac{\partial^2\psi_2}{\partial z^2} \tag{3.29}$$

$$\frac{1}{\alpha_\psi}\frac{\partial\psi_1}{\partial t} = \zeta_3 + \frac{\partial^2\psi_3}{\partial x^2} + \frac{\partial^2\psi_3}{\partial y^2} + \frac{\partial^2\psi_3}{\partial z^2} \tag{3.30}$$

3.5.5.velocity equation

$$U = \frac{\partial\psi_3}{\partial Y} - \frac{\partial\psi_2}{\partial Z} \tag{3.31}$$

$$V = \frac{\partial\psi_1}{\partial Z} - \frac{\partial\psi_3}{\partial X} \tag{3.32}$$

$$W = \frac{\partial\psi_2}{\partial X} - \frac{\partial\psi_1}{\partial Y} \tag{3.33}$$

3.6 Heat transfer

One of the main objectives of studying natural convection in an enclosure is to determine the rate of heat transfer .It thus involves the heat transfer into

and out of the enclosure. Generally the heat flows from the hot surface to the cold surface.

For practical emphasis, heat transfer is directed at the average Nusselt number.

On the total non-dimensional heat transfer Θ, the effect of the fluid motion entering enclosure through the heated portion of the driving wall is an average Nusselt number namely:

$$\overline{Nu} = -\int\int \frac{\partial \Theta}{\partial n} dA$$

Where

$\frac{\partial \Theta}{\partial n}$ is the local Nusselt number.

CHAPTER FOUR

4.1 The numerical solution method

The systems of non-linear partial differential equations with appropriate boundary condition present in chapter three were solved using finite difference technique.

The method of false transient is used to convert the equations from elliptic to parabolic form by addition of false transient derivative. This allows the solution to be marched through time and later the equations are approximated using the Samarkic Andreyev ADI scheme.

4.2 The method of false transient

This method involves the insertion of a frictious transient term to the energy equation. Then the time derivative in the energy and momentum equations is modified by the inclusion of the false transient coefficient. The false transient coefficients used are $\frac{1}{\alpha_\theta}$, $\frac{1}{\alpha_\psi}$ and $\frac{1}{\alpha_\zeta}$.

The rationale behind having the transient terms i. e α_θ, α_Ψ, α_ζ is that faster convergence rates may be achieved with careful adjustment of these coefficients. The selection of the transients α's determined the effective time

step at which each equation is advanced i .e the smaller the α, the smaller time step. It is however unfortunate that the choice of α's cannot be determined a-priori. However, typical values are $\alpha_\theta = 2.0, \alpha_\Psi = 1.0$ and $\alpha_\zeta = 0.09$.

This is because the energy equation is the most stable, while the vorticity transport equation is the most unstable. On introduction of the false transients variables, it was assumed that the steady state solution is independent of transient path.

4.3 Mesh definition and notation

The solution region is divided into rectangular elements and the mesh points are denoted by dots in the figure below:

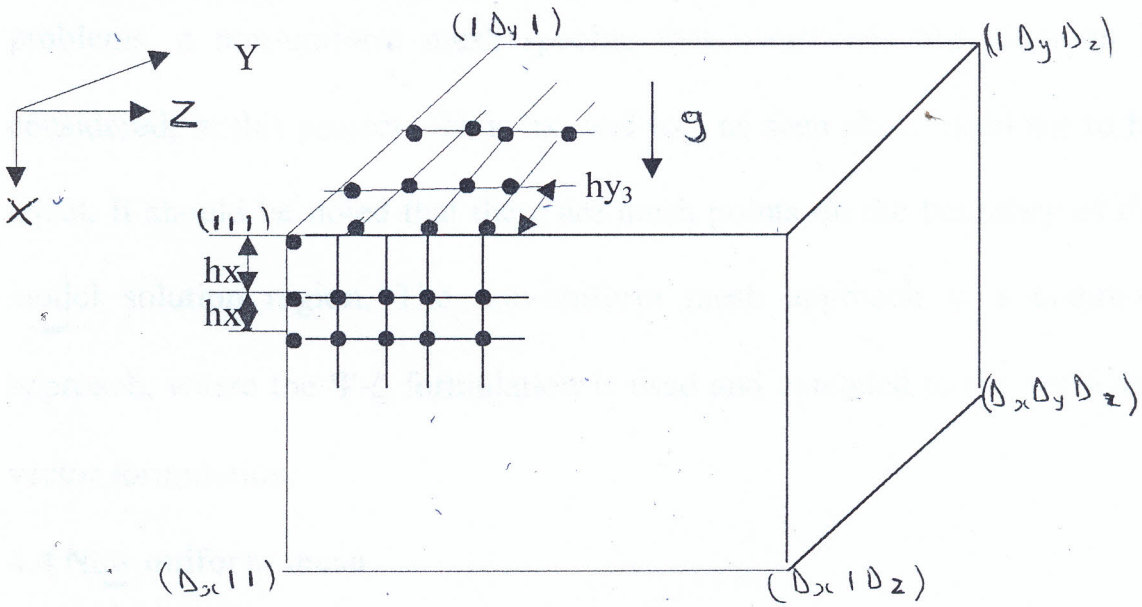

Figure 4.1 Mèsh notation

The value of all the variables (i.e ζ , Ψ, ν, θ) are calculated at the mesh points. The number of nodes in the x, y and z direction are D_x,D_y and D_z respectively and hx_I, hy_j and hz_k are the mesh spacing. The most common mesh pattern is the uniform grid, where the nodes are equally spaced throughout the solution region of interest. However, this grid pattern has two main drawbacks. In problems with thin boundary layers, it is impractical to use a uniform grid which gives sufficient resolution in the boundary layer region due to computer storage limitations. If a uniform grid was used in such a problem, the computation time per iteration would be substantial. Phillip and Schmidt (1984) approximated that the computational time is proportional to the square of the number of nodes used. Because of these problems, a non-uniform mesh spacing that overcomes this situation is considered, in this project. Thus hx_1 and hx_2, as seen above need not to be equal. It should be noted that there are mesh points on the boundary of the model solution region. The non-uniform mesh approach is a common approach, where the Ψ-ζ formulation is used and extended to the vorticity-vector formulation.

4.4 Non-uniform mesh

In this approach, grid spacing are varied through the solution space. Smaller spacing in regions where the flow gradients are high and larger spacing in

regions where the flow gradients is not changing significantly. Finite difference approximations to the governing equations are then developed, noting that the grid spacing is not uniform.

Magnus and Yoshihara (1970) concluded that this approach results in the use of fewer mesh points, which in turn results in a reduction of computer resources used.

Important factors related to the use of non-uniform mesh spacing are the orthogonality of the mesh pattern and the truncation error due to finite difference approximation. Care must however be taken when specifying grid spacing, because if the stretching is excessive, then the error due to the truncation terms would be large (i. e of order o(h)) Crowder and Dalton (1971).

In applying the finite difference to the partial differential equations, mesh points variables will be denoted by

$$\phi = \phi^{n}_{i,j,k}$$

$$\phi = \phi_{i+1,j,k}$$

4.4.1 Truncation error

When a uniform mesh is used, the approximation to the first and second derivatives using a three-point central difference approximation results in a truncation error of order o(h),

When a non-uniform mesh is used however, the truncation error for the second derivative may deteriorate to $0(h^2)$. To guarantee $0(h^2)$, truncation error for the second derivative when using non-uniform mesh, the expansion ratio are kept small and vice versa (Gatheri *al et.* 1994).

The numerical accuracy depends not only on having many grid points in the region of high gradients but also the grid points need to be approximately equally spaced as well.

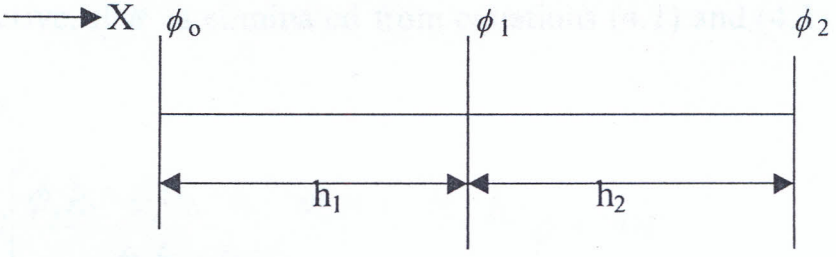

Figure 4.2 Three point difference approximation

Using a Taylor series expansion about points 0 and 2 in the above figure yields,

$$\phi_2 = \phi_1 + h_2\phi' + \frac{h_1^2}{2}\phi'' + \frac{h_2^3}{6}\phi''' \qquad (4.1)$$

$$\phi_0 = \phi_1 - h_1\phi' + \frac{h_1^2}{2}\phi'' - \frac{h_2^3}{6}\phi''' \qquad (4.2)$$

Eliminating ϕ'' from above and rearranging the terms yields

$$\phi' = \frac{\phi_2 h_1^2 - \phi_1 (h_1^2 - h_2^2) - \phi_0 h_2^2}{h_2 h_1^2 + h_1 h_2^2} + \frac{1}{6}\left(\frac{h_2^3 h_1^2 + h_1^3 h_2^2}{h_1 h_1^2 + h_1 h_2^2}\right)\theta''' + HOT$$

Which in turn yields

$$\phi' = \frac{\phi_2 h_1^2 - \phi_1 (h_1^2 - h_2^2) - \phi_0 h_2^2}{h_2 h_1^2 + h_1 h_2^2} + 0(h^2) \text{ term} \tag{4.3}$$

Thus the truncation error for the first derivative is always $0(h^2)$.

Now considering the finite difference approximation to the second derivative, if θ' is eliminated from equations (4.1) and (4.2) and rearranged, yields

$$\phi'' = 2\left[\frac{\phi_0 h_2 - \phi_1 (h_1 + h_2) + \phi_2 h_1}{h_2 h_1^2 + h_1 h_2^2}\right] + \frac{(h_1 - h_2)}{3}\phi''' + HOT$$

Which basically is of first order

Considering the ϕ''' term i.e the truncation error:

Let

$h_2 = h_1 + \alpha h_1$

$\therefore \frac{1}{3}(h_1 - h_2) = \frac{1}{3}(h_1 - h_1 - \alpha h_1)$

$= -\frac{1}{3}\alpha h_1$

Where α determines the degree of stretching.

Thus the truncation error is of order $0(h^2)$ if α is of the same order as h

For an example, consider a one-dimensional problem with 41 nodes:

A typical step size $(h_1) = \frac{1}{40} = 0.025$

Let $\alpha = 0.1$

$\therefore$ the truncation error $= -\frac{1}{3}\alpha h_1 \theta'''$

$$= -\frac{1}{3}(0.1)(0.025)\theta'''$$

$$= -8.33 \times 10^{-4}.\theta'''$$

$$= -(0.0288)^2.\theta'''$$

$$= 0(h^2)$$

Note

As the number of nodes is increasing, the truncation error due to grid stretching decreases. Since the truncation error is dependent on the number of nodes used as well as the degree of stretching, the truncation error has to be calculated for each grid pattern to ensure that it is acceptable.

Thus the three-point central difference scheme has been used in this project with the above restriction placed on the mesh stretching.

4.5 Summary of Finite Difference Approximation

The three point central difference approximations to the first and second derivatives developed in the previous section will now be summarized.

Using central difference about point i, gives

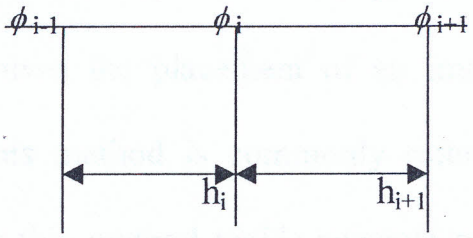

Figure 4.3 Three point central difference

$$\phi' = c_3\phi_{i+1} + c_2\phi_i + c_1\phi_{i-1} \tag{4.4}$$

Where:

$$c_3 = \frac{h_i^2}{\left(h_{i+1}h_i^2 + h_i h_{i+1}^2\right)}$$

$$c_2 = \frac{-\left(h_i^2 - h_{i+1}^2\right)}{\left(h_{i+1}h_i^2 + h_i h_{i+1}^2\right)}$$

$$c_1 = \frac{-h_{i+1}^2}{\left(h_{i+1}h_i^2 + h_i h_{i+1}^2\right)}$$

and

$$\phi'' = c_6\phi_{i+1} + c_5\phi_i + c_4\phi_{i-1} \tag{4.5}$$

where

$$c_6 = \frac{2h_i}{\left(h_{i+1}h_i^2 + h_i h_{i+1}^2\right)}$$

$$c_5 = \frac{-2\left(h_i + h_{i+1}\right)}{\left(h_{i+1}h_i^2 + h_i h_{i+1}^2\right)}$$

$$c_4 = \frac{2h_{i+1}}{\left(h_{i+1}h_i^2 + h_i h_{i+1}^2\right)}$$

When solving for points at the boundary, using three-point difference approximation involves the placement of an imaginary node outside the solution region. This method is commonly referred to as "mirror image technique". Though this method yields accurate results, it requires that the boundary condition to be implicitly incorporated into the equation being solved. This is easily implemented when a particular boundary is subjected to only one set of conditions. An example is the vector potential where the tangential components and the normal derivative of the normal component is zero at the boundary.

However when solving for temperature at the boundary for example, there is more than one set of conditions that exist and the implementation of the mirror image technique becomes cumbersome. Thus a three-point forward difference scheme will be used instead, in such a case. This method has the advantage of being highly flexible and ease in programming.

Using a similar technique to that which was presented in section 4.5, the first derivative may be approximated using forward differences.

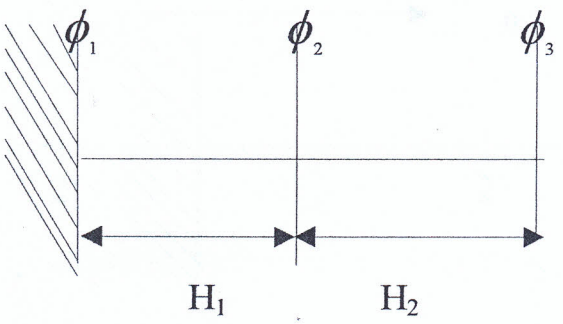

Figure 4.4 Three point forward difference:

$$\phi' = c_1\phi_1 + c_2\phi_2 + c_3\phi_3 \tag{4.6}$$

Where

$$c_1 = \frac{-\left[(h_1+h_2)^2 - h_1^2\right]}{\left[h_1(h_1+h_2)^2 - (h_1+h_2)h_1^2\right]}$$

$$c_2 = \frac{\left[(h_1+h_2)^2\right]}{\left[h_1(h_1+h_2)^2 - (h_1+h_2)h_1^2\right]}$$

$$c_3 = \frac{-h_1^2}{\left[h_1(h_1+h_2)^2 - (h_1+h_2)h_1^2\right]}$$

4.6 Finite Difference formulation of boundary conditions

4.6.1 Temperature boundary condition

The model developed in this project could allow four different types of temperature boundary conditions. These are isothermal, heat flux, adiabatic and convective surface conditions. However the present results have been obtained with the assumption that all the remaining walls are adiabatic.

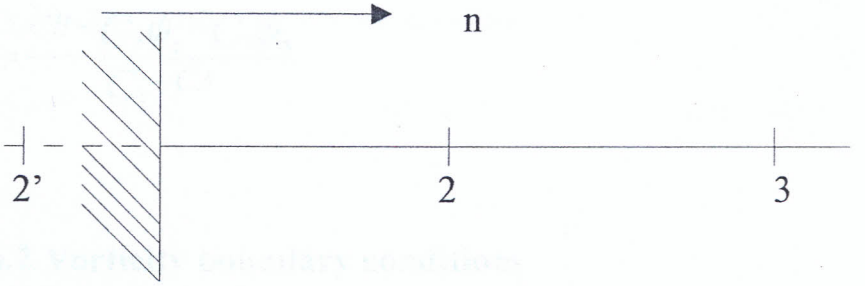

Figure 4.5 Thermal boundary conditions (sketch)

All other derivative boundary conditions may be expressed as,

$$\frac{\partial \phi}{\partial n} = CA.\phi 1 + CB \tag{4.7}$$

If CA=CB=0, the boundary is adiabatic.

Equation 4.7 can be solved for ϕ_1 by either using central differences about point 1(i. e the mirror image) or forward differences from point 1.

Although the former yields more accurate results than the latter, it requires that the boundary condition to be implicitly incorporated into the equation being solved. Thus the more flexible three-point forward difference scheme has been used.

Applying a three point forward difference to equation (4.7) yields,

$$C_1\phi_1 + C_2\phi_2 + C_3\phi_3 = CA.\phi_1 + CB \tag{4.8}$$

Where C1, C2 and C3 are given in section 4.2.2

Rearranging equation (4.8) yields

$$\phi_1 = \frac{CB - C_2\phi_2 - C_3\phi_3}{C_1 - CA}$$

4.6.2 Vorticity boundary conditions

Woods (1954) obtained the finite difference approximation of the vorticity boundary condition in two dimension. Later Mallinson (1973) successfully extended this method to three dimensions from a Taylor's series expansion of the equation $\zeta = -\nabla^2\psi$ .This equation is valid at the wall and using n to represent the coordinate normal to the wall , the vorticity between the wall and the first internal point (see figure 4.6) may be approximated as:

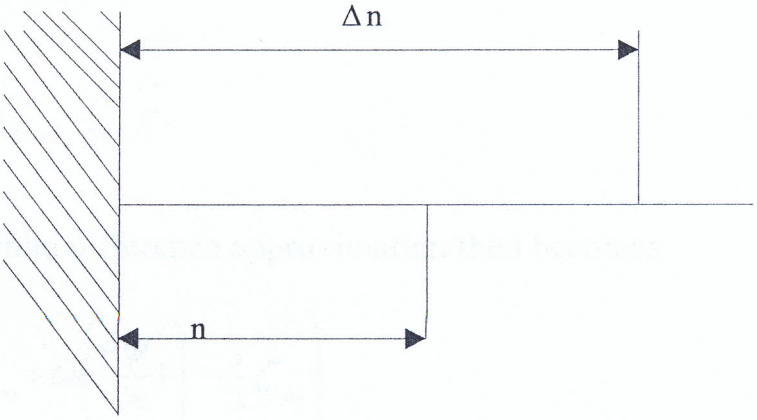

Figure 4.6 vorticity boundary conditions (sketch)

$$\zeta_{n1} = -\left(\frac{\partial^2 \psi_n}{\partial n^2}\right)_1 \qquad (4.9)$$

Where the subscript '1' denotes the mesh point on the wall. Applying a Taylor's series expansion for ψ_n in n about the mesh point on the wall yields

$$\zeta_{n1} = \frac{2}{\Delta n^2}\left[\psi_{n2} - \Delta n\left(\frac{\partial \psi_n}{\partial n}\right)\right] + \frac{\Delta n}{3}\left(\frac{\partial^2 \psi_n}{\partial n^2}\right) + HOT \tag{4.10}$$

Where Δn is the mesh interval between the wall and the first mesh point. Applying equation (4.9), the term $\frac{\partial^3 \psi_n}{\partial n^3}\left(\frac{\Delta n}{3}\right)$ may be written as

$$-\frac{\Delta n}{3}\left(\frac{\partial \zeta_n}{\partial n}\right) - \frac{\Delta n}{3}\left(\frac{\partial \zeta_n}{\partial n}\right) \tag{4.11}$$

Expanding ζ_n about the mesh point on the wall yields

$$\frac{\Delta n}{3}\left(\frac{\partial \zeta_n}{\partial n}\right)_1 = \frac{1}{3}\left(\zeta_{n2} - \zeta_{n1}\right) \tag{4.12}$$

The vorticity finite difference approximation then becomes

$$\zeta_{n1} = \frac{3}{\Delta n^2}\left(-\psi_{n2} + \Delta n\left(\frac{\partial \psi_n}{\partial n}\right)_1 - \frac{1}{2}\zeta_{n2}\right) \tag{4.13}$$

The term $\left(\frac{\partial \psi_n}{\partial n}\right)_1$ is evaluated using the definition of the vector potential i,e

$\hat{V} = \nabla \times \hat{\psi n}$

4.6.3 Vector potential boundary conditions

In section 3.3.3 it was shown that there are two conditions for the vector potential at the boundary.

$$\psi_{t1}\psi_{t2} = 0 \qquad (4.14a)$$

$$\frac{\partial \psi_n}{\partial n} = 0 \qquad (4.14b)$$

Application of the (4.14a) is trivial while the (4.14b) may be implemented using either mirror image or three point forward difference. Unlike the boundary conditions for temperature, the second condition is general since it represents the impermeability condition and therefore the more accurate mirror image method will be used.

In applying the mirror image method, an imaginary point is created outside the solution region, as shown in the figure below:

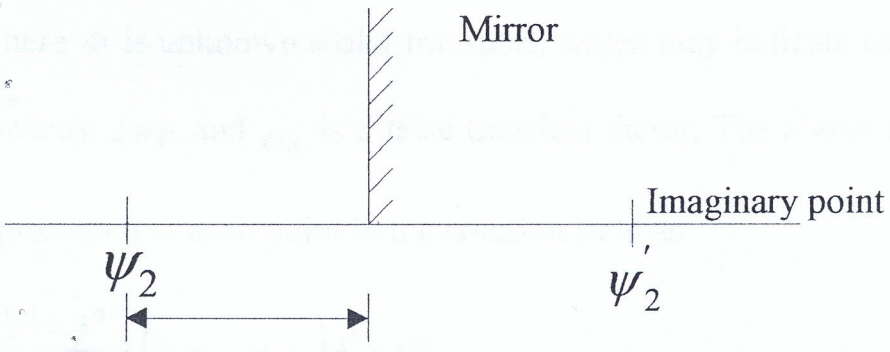

Figure 4.9 Mirror image

The boundary condition is written as,

$$\frac{\partial \psi_n}{\partial n} = \frac{\psi_2' - \psi_2}{2h} = 0 \tag{4.15}$$

and hence

$$\psi_2' - \psi_2 = 0 \quad \text{or} \quad \psi_2' = \psi_2 \tag{4.16}$$

Equation (4.15) is then incorporated into the solution procedure for the vector potential.

4.7 The ADI scheme

The time dependent parabolic equation may be advanced through a sequence discrete time intervals over which each equation may be linearised that all variables other than that in the $\frac{\partial}{\partial t}$ term are independent of time. The general form of this family of equation may be given as

$$\frac{1}{\alpha_\phi}\frac{\partial \phi}{\partial t} = f\left(U, V, W, \nu\, \zeta_1 \zeta_2 \zeta_3 \Theta\right) \tag{4.17}$$

Where Φ is unknown scalar transport, which may indicate the component of vorticity $\zeta or \phi$ and α_ϕ is a false transient factor. The above equation can be represented at each point in the solution field as

$$\frac{\phi^{n+1} - \phi^n}{\alpha_\phi} = \left(a_x + a_y + a_z\right)\phi^n + S_\phi^n \tag{4.18}$$

where $a_x a_y and a_z$ are point operators representing the finite difference approximation to the derivatives as indicated by the subscripts and S_ϕ^n is a source term. If ϕ is written as a vector of the mesh point and A_x, A_y and A_z are matrices consisting of the point operators a_x, a_y and a_z, equation (4.17) may be written as

$$\frac{\{\phi\}^{n+1} - \{\phi\}^n}{\alpha_\phi \Delta t} = \left(A_x + A_y + A_z\right)\{\phi\}^n + \{S_\phi\}^n \tag{4.19}$$

Which can be rearranged as

$$\{\phi\}^{n+1} = \{\phi\}^n + \alpha_\phi \Delta t\left(A_x + A_y + A_z\right)\{\phi\}^n + \{S_\phi\}^n \tag{4.20}$$

By considering equation (4.18) the working of the Sarmarski-Andreyev (ADI) scheme can be established. Surpose that

$$\{k\} = \frac{\{\phi\}^{n+1} - \{\phi\}^n}{\alpha_\phi \Delta t} \tag{4.21}$$

and for a partial implicit scheme $\{\phi\}$ the right hand side of the equation (4.22) is replaced by

$$\delta\{\phi\}^{n+1} + (1-\delta)\{\phi\}^n \tag{4.22}$$

Where δ is a weighting factor. When $\delta = 1$ the method is fully implicit ,and $\delta = 0$ the method is fully explicit, and when $\delta = \frac{1}{2}$ the formulation reduces to Crank-Nicolson (1947) method.

Equation (4.19) hence reduces to

$$\{k\} = \left(A_x + A_y + A_z\right)\left(\delta\{\phi\}^{n+1} + (1-\delta)\{\phi\}^n\right) + \{s_\phi\}^n \tag{4.23}$$

From the above definition (4.20), $\{\phi\}^{n+1}$ can be expressed in terms of $\{\phi\}^n$ and $\{k\}$ so that equation (4.22) becomes

$$\{k\} = \left[A_x + A_y + A_z\right]\left[\delta_\phi \delta\Delta t\{k\} + \{\phi\}^n\right) + \{s_\phi\}^n \tag{4.24}$$

Which when rearranged gives

$$\left\{I - \alpha_\phi \delta\Delta t\left(A_x + A_y + A_z\right)\right\}\{k\} = \left(A_x + A_y + A_z\right)\{\phi\}^n + \{s\}^n \tag{4.25}$$

In which I is the identity matrix. The right hand side of (4.25) is known, hence $\{k\}$ can be evaluated and $\{\phi\}^{n+1}$ can be obtained from equation (4.21) by rearranging it as

$$\{\phi\}^{n+1} = \{k\}\alpha_\phi \Delta t + \{\phi\}^n$$

Solving equation (4.25), inversion of the tri-diagonal matrix $\left\{I - \alpha_\phi \delta\Delta t\left(A_x + A_y + A_z\right)\right\}$ becomes necessary. This can be attained by applying the ADI scheme which can be written as

$$\left(I - \alpha_\phi \delta\Delta t\, A_x\right)\{k\}^* = \left(A_x + A_y + A_z\right)\{\phi\}^n \tag{4.26a}$$

$$\left(I - \alpha_\phi \delta\Delta t\, A_y\right)\{k\}^{**} = \{k\}^* \tag{4.26b}$$

$$\left(I - \alpha_\phi \delta\Delta t\, A_z\right)\{k\}^{***} = \{k\}^{**} \tag{4.26c}$$

where * is the intermediate value in the ADI scheme.

The inversion of the tri-diagonal matrices of 'locally one-dimensional implicit equation (4.25) is solved using the highly efficient Thomas algorithm (Thomas 1949) in each direction.

4.8 solution of parabolic equations

The finite difference approximation to the equations in chapter three i .e partial differential equations in component form may be solved in a variety of ways. For example if we consider the i-component of the vorticity-vector potential equation (3.28) viz,

$$\frac{1}{\alpha_\psi}\frac{\partial \psi_1}{\partial t} = \zeta_1 + \frac{\partial^2 \psi_1}{\partial x^2} + \frac{\partial^2 \psi_1}{\partial y^2} + \frac{\partial^2 \psi_1}{\partial z^2} \tag{4.27}$$

Using the finite difference approximation for the first and second derivatives, this becomes:

$$\frac{1}{\alpha_\psi}\frac{\partial \psi_1}{\partial t} = \zeta_1 + \delta_{xx}\psi_1 + \delta_{yy}\psi_1 + \delta_{zz}\psi_1 \tag{4.28}$$

where δ_x is the finite difference approximation to $\frac{\partial}{\partial x}$

δ_{xx} is the finite difference approximation to $\frac{\partial^2}{\partial x^2}$

Equation (4.27) can be solved using explicit methods such as the Dufort-Frankel method or point iterative methods such as the Gauss-seidel iteration. However (A D I) methods are the most widely used in solving

numerical fluid dynamics problem. In these methods, each time step is subdivided into three levels in the case of a three dimensional problem. The A D I scheme which has been implemented in this project is the samarakii-Andreyev scheme.

4.9 Finite difference equation in implicit form

Equation 4.30 has been written implicit in the x, y and z directions to allow the one-dimensional equations to be solved using the highly efficient Thomas algorithm (de Vahl Davis (1976))

ψ_1 , in the right hand side of equation (4.30) can be replaced by,

$$\psi_1 = \sigma \psi_1^{n+1} + (1-\sigma)\psi_1^n \qquad (4.29)$$

where σ is a weighting factor, between 0 and 1. I f $\sigma = 0.5$, this becomes an extension of the crank-Nicholson scheme (1947). Equation (4.29) can be further manipulated as,

$$\psi_1 = \alpha_\psi \sigma \Delta t \omega + \psi_1^n .$$

In which,

$$\omega = \frac{\psi_1^{n+1} - \psi^n}{\alpha_\psi \Delta t} \qquad (4.30)$$

where α_ψ is a false transient factor and Δt is the time step.

Substitution of equation (4.30) into equation (4.29) yields

$$\omega = \zeta_1 + \alpha_\psi \sigma \Delta t \left(\delta_{xx}\omega + \delta_{yy}\omega + \delta_{zz}\omega\right) + \delta_{xx}\psi_1^n + \delta_{yy}\psi_1^n + \delta_{zz}\psi_1^n \qquad (4.31)$$

The Samarskii-Andreyev scheme now involves decomposing equation (4.30) into three one-dimensional equations;

Implicit in x:

$$\omega^* + \alpha_\psi \sigma \Delta t \left(-\delta_{xx}\omega^*\right) = \delta_{xx}\psi_1^n + \delta_{yy}\psi_1^n + \delta_{zz}\psi_1^n + \zeta_1 \qquad (4.32a)$$

where ζ_1 is known as the source term for this equation;

Implicit in y:

$$\omega^{**} + \alpha_\psi \sigma \Delta t \left(-\delta_{yy}\omega^{**}\right) = \omega^* \qquad (4.32b)$$

Implicit in z:

$$\omega^{***} + \alpha_\psi \sigma \Delta t \left(-\delta_{zz}\omega^{***}\right) = \omega^{**} \qquad (4.32c)$$

and the updated value is given by:

$$\psi_1^{n+1} = \psi_1^* + \alpha_\psi \Delta t\, \omega^{***} \qquad (4.33)$$

Equations (4.32a), (4.32b) and (4.32c) are the three one-dimensional equations, each to be solved implicit at the x y and z levels respectively. The value of ψ_1 at the new time step, n+1, is then evaluated using equation (4.33).

4.10 Solution procedure.

The solution methods in the last section are designed to handle only one problem in isolation, therefore the solution to the set of difference equation must be sought by iterative method.

In this section a summary of the solution procedure to solve the five equations (ζ_1 , ζ_2 , ζ_3 , Ψ, Θ) is given. The procedure is marched through time until convergence

1: Initialisation of all the variables and constants.

2: The components of the vector-potential are solved iteratively to convergence over one time step

3: Calculation of the velocity from the vector potential is obtained.

4: The components of the vorticity transport equation are solved using the ADI scheme.

5: Updating of the boundary conditions for vorticity is done.

6: Solving energy equation using the ADI scheme.

7: Updating the boundary conditions for the energy equation.

The procedure is repeated until convergence is obtained and the results printed, however the process shall terminate when the iteration exceeds a specific value.

The above procedure has omitted details such as reading the input variables (e. g Ra) and halting the solution procedure when the solution has diverged.

4.11 Stability, convergence and divergence

A solution is deemed to have converged when a steady state has been reached. It is said to be in stead state when the value of the variables (e.g.Θ) from one time step to another does not change. In a numerical procedure a criterion must be defined to measure the rate of change of the solution. A commonly used criterion is by de Vahl Davis (1976), which represents the normalized averaged effective time rate of change of the variable considered This is given by ,

$$C \geq \frac{\sum_{i=1}^{NX}\sum_{j=1}^{NY}\sum_{k=1}^{NZ}\left|\frac{\Theta^{n+1}-\Theta^{n}}{\alpha_{\phi}\Delta t}\right|}{NX.NY.NZ\max\left(|\Theta|\right)}$$

where c is the convergence criterion for Θ . When the values of the variables exceed a chosen value (e.g. 1000 for ξ ,Ψ or Θ exceeds 1) then the solution is said to have diverged.

CHAPTER FIVE

Laminar natural convection in a rectangular enclosure

5.1 Introduction

Localized heating and cooling causes non-uniformity in the boundary temperature of a single vertical wall resulting in a colliding boundary condition. The geometry of the problem of interest in this project has been outlined in chapter three. The rest of the walls have been assumed to be insulated .The heater area has been kept constant and location fixed. It is the purpose of this study to investigate the resultant thermal and flow fields and the rates of heat transfer. Locallised heating and cooling include two boundary layers that collide in the region between the window and the heater hence we concentrate on the resultant flow fields.

In many enclosures (room), both forced and free convection play an important role in the determination of the air movement and heat transfer of the indoor climate. The enclosure considered in this work is assumed to have no fans and no inlets or outlets so that the flow is driven by buoyancy alone. Although many heaters project from the wall, forming a passage between the wall and the heater, in this study it is assumed that both the window and the heater are built flush with the wall. Under winter conditions heat is usually

transferred through the windows to the environment while the heater provides a heat input to counter this loss.

5.2 The geometry and results discussion.

In the present study the effects of the existence of a cold isothermal window and a hot isothermal heater of equal height along a single vertical wall in an enclosure is investigated. The results have been obtained by solving the vorticity transport equations and the energy equation together with the various boundary conditions using a highly scientific fortran 77 computer code. It is shown that the natural convection phenomenon evolving in the enclosure differs fundamentally from the well-known results for the model, which assumes that the two opposite vertical walls of the cavity are differentially heated (Ostrach 1982, Bejan (1984)). In the enclosure when the heater and the window are set on simultaneously, two large, equally sized, counter-rotating rolls are formed. The upper roll, driven by the cold surface, and the lower roll, driven by the hot surface (Poulikakos (1985)).

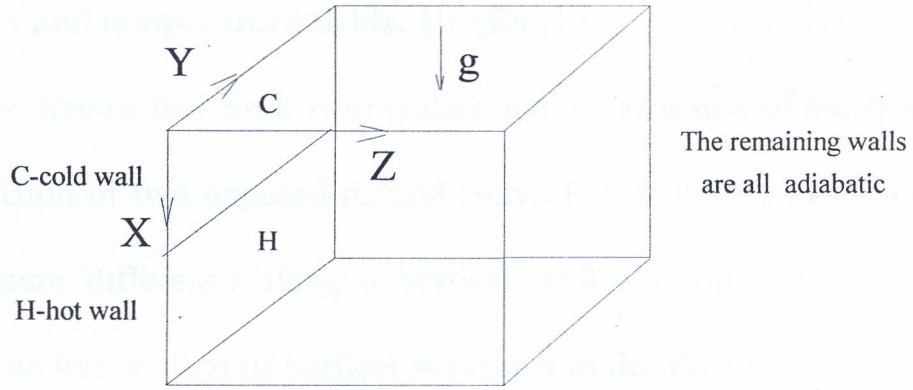

Figure 5.1 The schematic diagram for the case of colliding boundary layers with buoyancy effects.

As mentioned earlier the Rayleigh number considered in this project was $Ra > 5\times10^5$, and as such, a numerical solutions could not be obtained with a conventional false transient factor method. Only when the variable false transient factors formulation was employed could solutions be obtained.

Thus the variable false transient factors has been used to maintain the stability of the solution procedure and hence obtain converged solutions in a reasonable time. This has resulted with converged solution for Rayleigh number that was not possible when using the conventional false transient method. However, the results for the highest Rayleigh number in the present study ($Ra=10^6$) show increased waviness of the flow along the horizontal mid-height.

5.3 Flow and temperature fields: $10^5 \leqslant Ra \leqslant 10^6$

The objective of this work is to understand the structure of the flow due to the collision of two opposed natural convection boundary layers driven by temperature difference along a vertical wall and the mechanism which causes the formulation of vortical structures in the flow that jets away from the wall. Solutions have been obtained for the Rayleigh number $10^5 \leqslant Ra \leqslant 10^6$ and Pr=0.71.

For easy analysis of the results, all the vector plots shall be referred as CASE 1 and the isotherms, CASE 2.

CASE 1

To reveal the fine structure of the thermal boundary layers, most of the vector plots in the x-z plane have been selected on the symmetry plane and near the side wall. In the case of the x-y plane the vector plots near the active wall and at the rear of the enclosure where most of the flow is concentrated have been selected. Vector plots in the y-z plane have been selected along the borderline between the heater and window and at the centre of the cold and hot rolls. Particle tracks are used to depict the flow structure in the lower hot region and the upper cold region. Where the flow crosses from the lower hot to the upper cold region particle tracks have been used to trace the flow across the horizontal mid-plane.

The heating over the lower half and cooling over the upper half creates an unstable stratification of fluid at the colliding boundary layer. At sufficiently high Rayleigh number (high temperature difference), a strong convective motion develops and heat is transferred from the lower half to the upper half. Fluid in the upper half moves so that the cold fluid descends adjacent to the walls and collides with the rising fluid from the lower half. This collision of the boundary layer takes place halfway between the vertical wall. After colliding, the boundary layers curve into the room and they join to form a horizontal jet that moves across the cavity as shown in Figures 5.2 and 5.3.

As shown in Figures 5.2 and 5.3, the collision and deflection of the boundary layers occur in the region where the cold and hot surface converges. The deflection of the boundary layers could be the result of a centrifugal instability as suggested by Floryan (1986). As illustrated in the figures, fluid from the cold region descends along the wall meeting the fluid from the lower half which rises along the wall. After collision, the two boundary layers curve into the room where they join to form a horizontal jet which penetrates into the enclosure. As the jet moves across the cavity, it breaks up into two counter rotating rolls which moves in opposite directions. One roll move upwards and returns to the cold window via the ceiling while another roll move downwards and returns to the heater via the floor of the

cavity. At any vertical cross-section the fluid motion appears to form closed paths. Fluid in the upper half of the cavity rotates in an anti-clockwise direction while the fluid in the lower side rotates in a clockwise direction. The upper roll, driven by the cold window, on average is slightly below the mean room temperature Θ_R. Along the horizontal mid-plane the dimensionless temperature is between 0.45 and 0.55.

Figure 5.3(a) shows an isometric view of the flow profile near the active wall and parallel to the heater and window surfaces, and at the symmetry plane. Near the rear wall the horizontal stream breaks up into two counter-rotating rolls, which move in opposite directions.

The flow profile across the cavity in the plane parallel to the heater and window is depicted in Figures 5.3(b) (see also Figure 5.2(b)). In these figures, the flow is shown near the active wall, at the centre of the cavity and near the rear wall. At the centre of the cavity, the flow near the ceiling and at the floor of the cavity moves towards the active wall where at the centre the flow move towards the rear wall. The above figure are in different view positions.

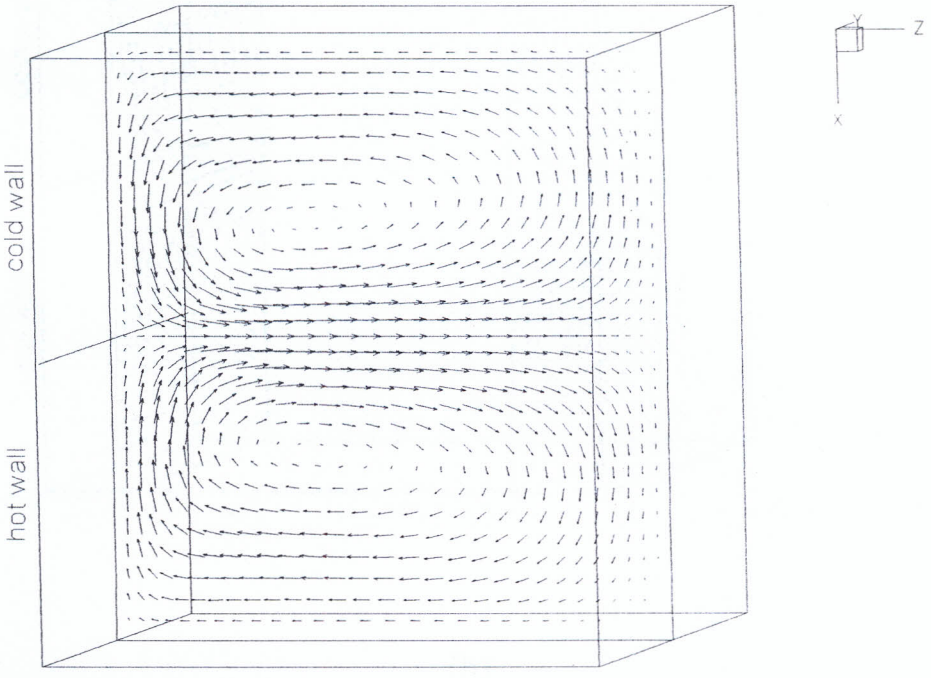

(a)

Figure 5.2 Velocity vector plots at $Ra = 10^5$: (a) mid-plane at y=0.5

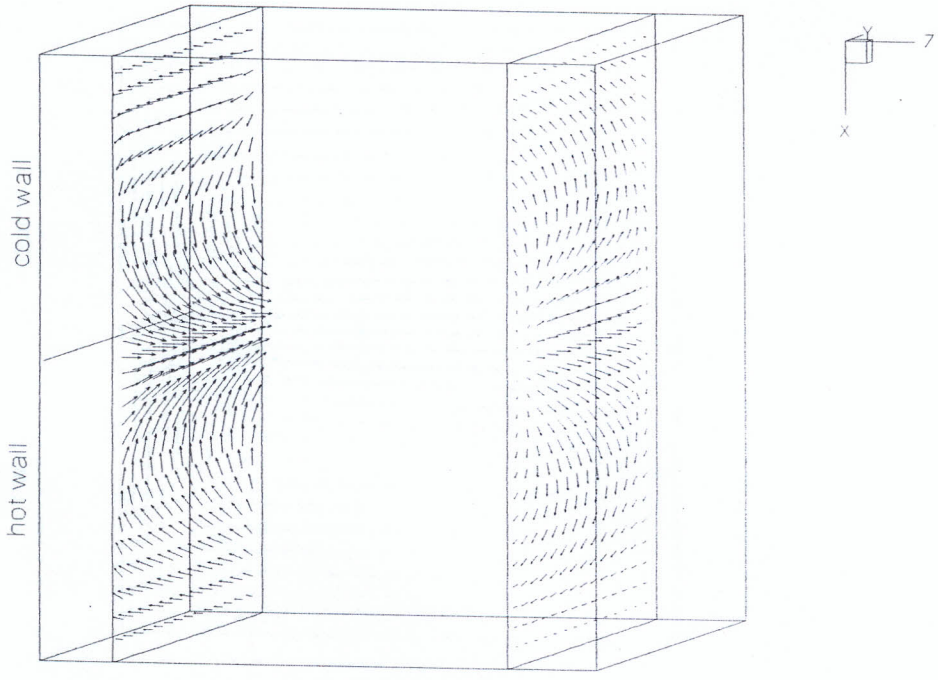

(b)

Figure 5.2 Velocity vector plots at $Ra = 10^5$: (b) end elevation at z=0.1 and z=0.9.

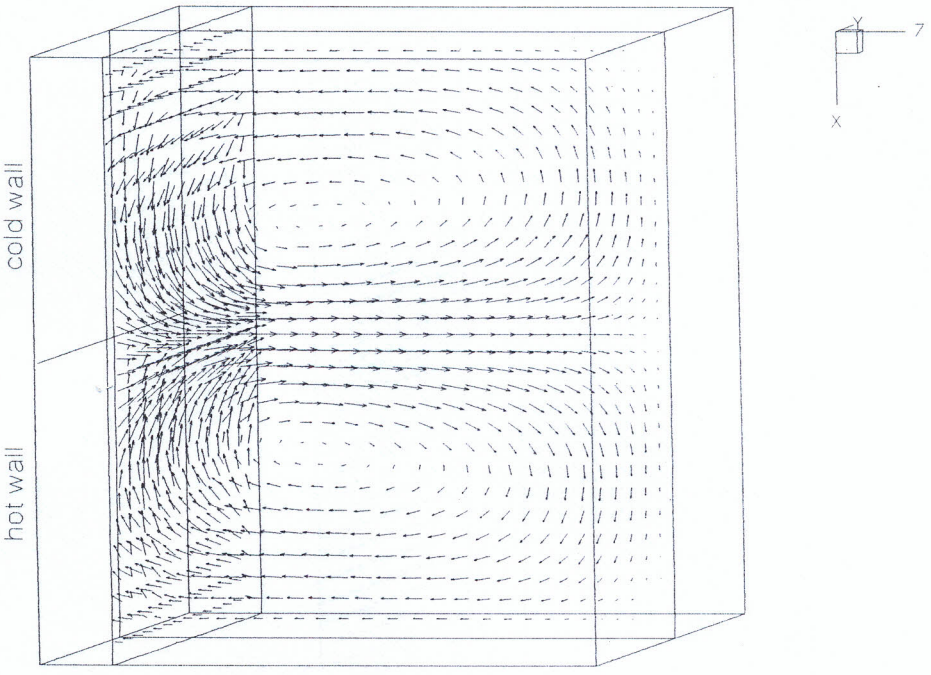

(a)

Figure 5.3 Velocity vector plots at $Ra = 10^5$: (a) isometric view at z=0.1 and y=0.5 and

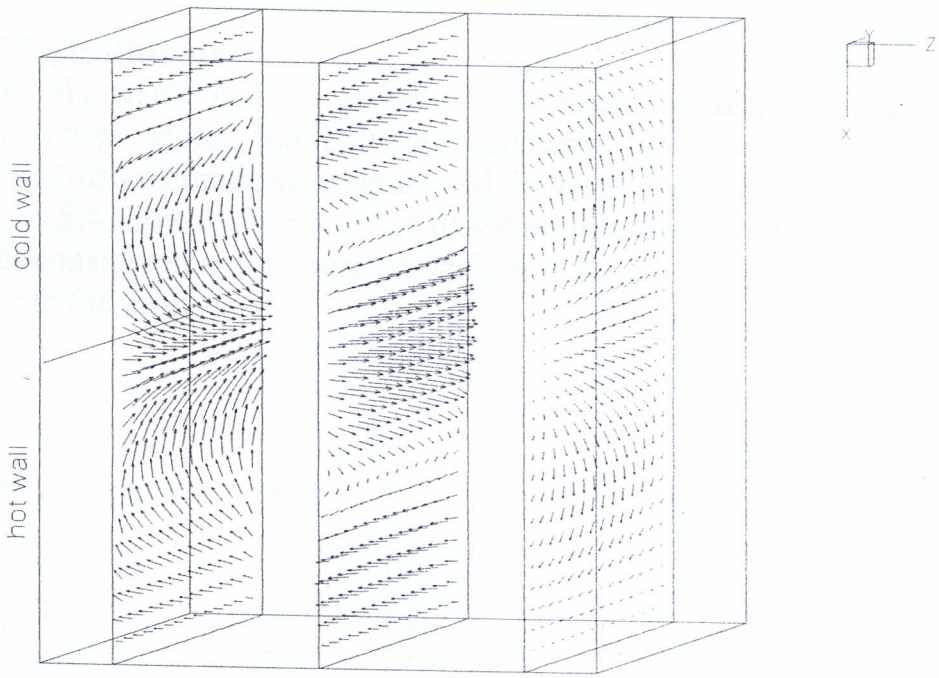

(b)

Figure 5.3 Velocity vector plots at $Ra = 10^5$: (b) end elevation at the planes z=0.1, z=0.5 and z=0.9 respectively.

CASE 2 Isotherms

In case 2 the results and discussion of the temperature distribution in the enclosure is presented. Similarly these isotherms have been generated by the scientific fortran computer program and the results bounded between 0 and 1.Figures 5.4 show the temperature distribution at the lowest Rayleigh number considered in this work while figures 5.5 are for the highest Raylegh number in the project.

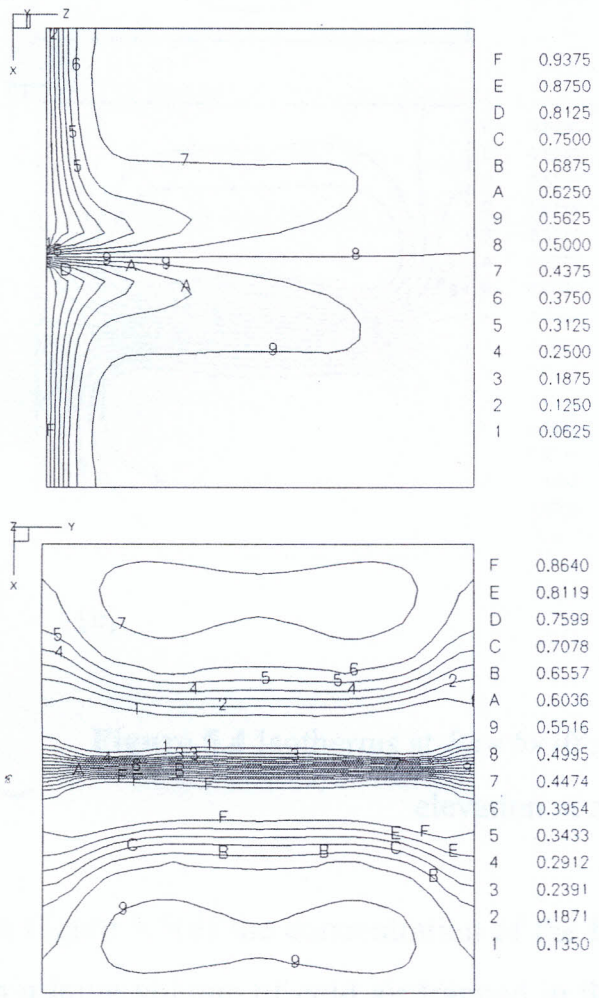

(a) (b)

Figure 5.4 Isotherms at $Ra = 5\times10^5$: (a) side elevation at y=0.5, (b) end elevation at z=0.1

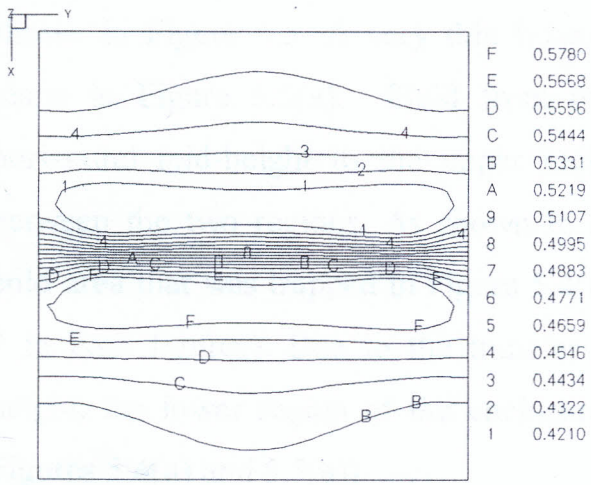

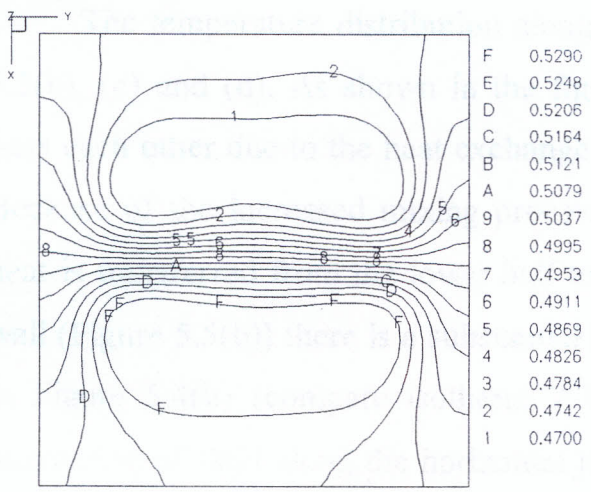

(c) (d)

Figure 5.4 Isotherms at $Ra = 5\times10^5$: (c) end elevation at z=0.5, (d) end elevation at z=0.9.

In Figure 5.5(d) the concentration of the flow along the horizontal jet results in a large volume of cold air trapped in the upper region and a similar large volume of hot air trapped in the lower region.

At Rayleigh number 5×10^6 the flow intensifies. In the case of the isotherms, there is a significant departure from the previous isotherms as

shown in Figure 5.5. A very thin boundary layer is evident along the x-z plane in Figure 5.5(a). Fluid from the lower region moves across the horizontal mid-height to the upper region. This results in heat exchange between the two regions. As shown in Figure 5.5(a), the larger volume of cold area that was trapped in Figure 5.4(a) has decreased (compare isotherm 7 in both figures). Due to the transfer of heat across the horizontal mid-height, the lower region of the enclosure is cooler (compare isotherm 9 in Figures 5.4(a) and 5.5(a)).

The temperature distribution along the x-y planes is shown in Figures 5.5(b), (c) and (d). As shown in the figures, hot and cold patches of fluid pass each other due to the heat exchange occurring between the two regions. Because of the increased mixing process taking place within the enclosure heat is transferred from the lower half to the upper half. Close to the active wall (Figure 5.5(b)) there is a substantial hotter fluid in the upper region than in Figure 5.4(b) (compare isotherm 7 in the two figures). The increased interaction of fluid along the horizontal jet is also indicated by the isotherms in Figures 5.5(b), (c) and (d).

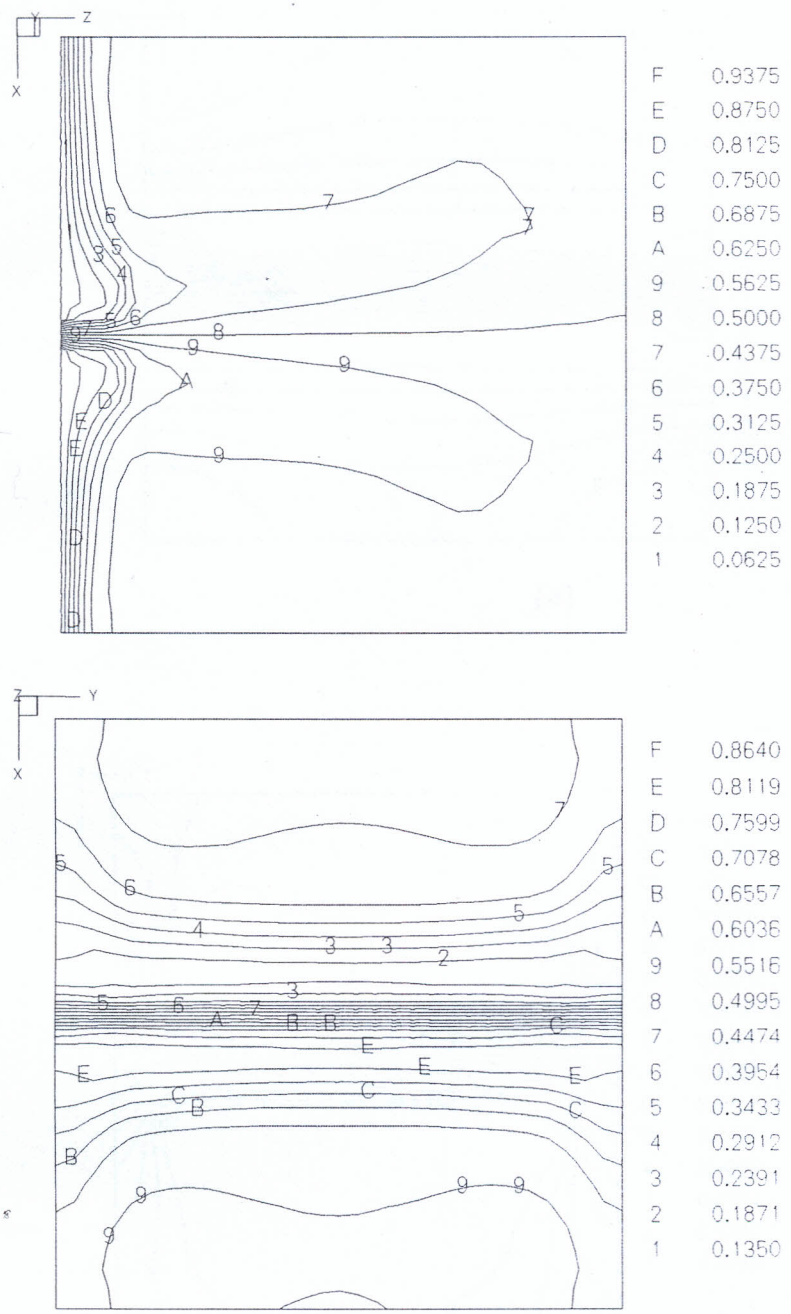

(a) (b)

Figure 5.5 Isotherms at $Ra = 10^6$: (a) side elevation at y=0.5, (b) end elevation at z=0.1

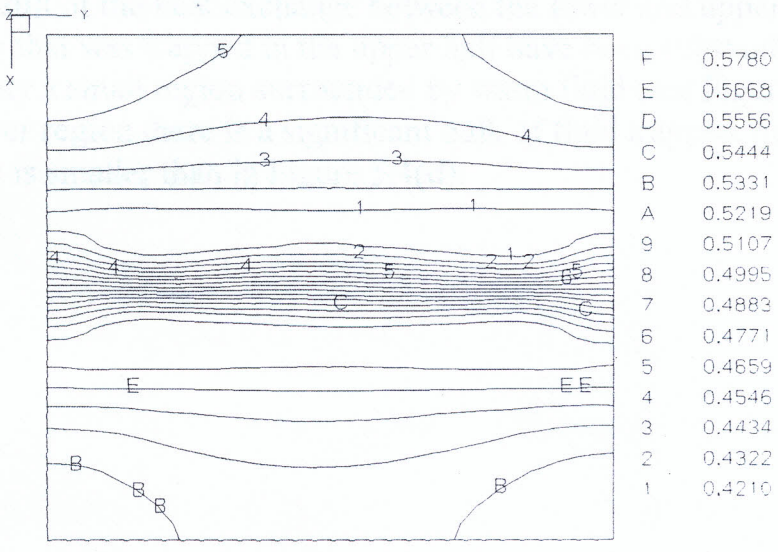

(c)

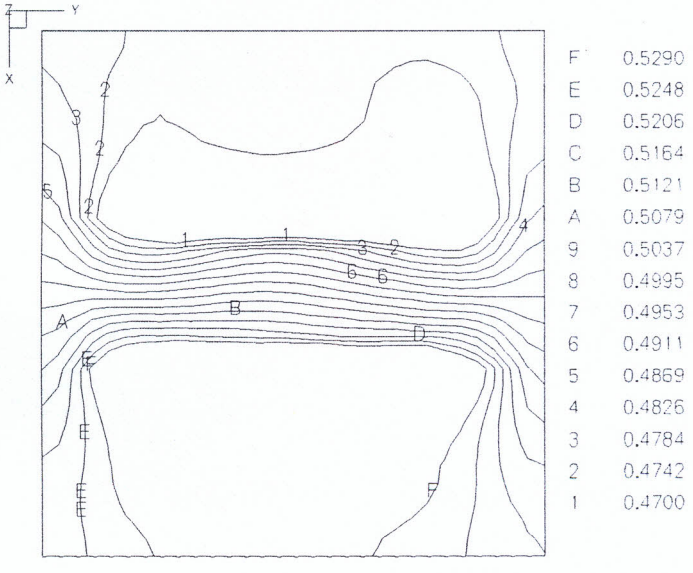

(d)

Figure 5.5 Isotherms at $Ra = 10^6$:(c) end elevation at z=0.5, (d) end elevation at z=0.9.

As a result of the heat exchange between the lower and upper region, the cold air that was trapped in the upper half have been substantially reduced with only a small region surrounded by warm fluid (see Figure 5.5(d)). In the lower region there is a significant bulk of fluid trapped, however the volume is smaller than in Figure 5.4(d).

CHAPTER SIX

1.1 Conclusion

The objective of this project was to understand the structure of the flow due to the collision of two opposed natural convection boundary layer driven by temperature difference along a vertical wall. Since it was natural convection problem the only internal force considered was the gravitational.

Solutions have been obtained for the Rayleigh number $10^5 \leqslant Ra \leqslant 10^6$ and Pr=0.71.

The geometry considered was a three-dimensional rectangular enclosure in form of a room containing a conventional heater mounted below a window.

A complete set of equations describing Newtonian fluid was presented in general form and later recast in vorticity/vector potential formulation, thus eliminating the need for solving the continuity equation.

The Boussinesq approximation was invoked, allowing the conservation equations to be simplified. As a result of this, when considering air field cavities the maximum allowable temperature difference is approximated 30K and for air field cavities it is 3K.

The governing equations with the boundary conditions were discretised using a three-point central difference approximation for a non-uniform

mesh. The resulting finite difference equations were then solved using the method of false transients and the Samarskii-Andreyev ADI scheme.

As a results it was found that the flow is dominated by collision of the boundary layers in the region halfway between the vertical walls and later curve into the room, joining to form horizontal jets which move across the enclosure. Collision and deflection occurs in the region where the cold and hot surfaces converge. This deflection could be as the result of a centrifugal instability as suggested by Floryan (1986). The results showed that the rate of heat transfer is moderate at low Rayleigh number and tends to increase substantial at higher Rayleigh numbers. Because of increased mixing process between the warm and cold fluid, where heat is transferred from the lower half to the upper half, it was found that there is less drought experienced in the enclosure. This is as a result of the heating and cooling in the same wall. These findings do agree with those found by de Vahl Davis (1986) where he realized strong drought is experienced when heating and cooling is not done on the same wall.

It is now clear that heating and cooling has a wide range of application in engineering as earlier on stated, hence need for more research efforts to the field is absolutely necessary. For my future extension of this work given

necessary resources, a more practical approach would be my focus of interest by reducing the many theoritical assumption made to achieve the current results. A systematic investigation of the heat transfer rates in an enclosure at various Rayleigh numbers and the applicability of various ranges of Rayleigh numbers is of much relevancy in my future reseach.

1.2 Recommendations for further research.

Due to time limitation, the following has been recommended as areas for research in future.

-Investigation of buoyancy-driven Laminar natural convection in an enclosure with various heater positions to determine the best location for maximum heat transfer rates.

-Though expensive in term of time and money as earlier stated, there is need for an Experimental approach to natural convection problems both at lower and higher Rayleigh numbers in order to validate the numerical results.

-Use of other numerical methods such as the finite element method to solve natural convection problems.

REFERENCES

1. Aziz, K and Hellums, J. D. (1967) "Numerical solution of the three dimensional equations of motion for laminar natural convection", The Phys. of Fluids. Vol 10.

2. Batchelor, G.K. (1967) "An introduction to fluid dynamics" Cambridge University Press.

3. Boussinesq, J (1903) "Theories analytique de la chaleur" Vol.2 Gauthier-villars, Paris.

4. Brandt, A . (1977) "Multilevel adaptive solutions to boundary value problems", Math Comp., Vol 31.

5. Brown, J. J. (1981) " A multigrid mesh-embedding technique for three dimensional transonic potential flow analysis", in H. Lomax (ed), Multi-grid methods, NASA Rept. 2202.

6. Cheung, H. F. and de Vahl Davis, G (1977) " Fourth order accurate numerical solutions of fluid mechanics problems", UNSW, School of Mech and Ind. Eng., Report FMT/3.

7. Currie, I. G. (1974) "Fundamental mechanics of fluids", Mc Graw-Hill Inc.

8. Crowder, H. J. and Dalton, C. (1971) "Errors in the use of non-uniform mesh systems", Journal of Comp. Physics, Vol 7.

9. Davis, S. H. (1967) "Convection in a box: linear theory", J. Fluid Mech.

10. de Vahl Davis, G. (1976) "Program Frecon – for the numerical solution of free convection in a rectangular cavity", UNSW, School of Mech. and Ind. Eng., Report FMT/1.

11. de Vahl Davis, G. and Wolfstein, M. (1974) "A study of a three dimensional free jet using the Vorticity/vector potential method", Int. conf. Num. Meth. In Fluid Dynamics.

12. de Vahl Davis, G. (1983) "Natural convection of air in a square cavity : A benchmark numerical solution, Int. J. Num. Meth. In Fluids, Vol 3.

13. de Vahl Davis, G. (1986) "Finite difference methods for natural and mixed convection in enclosures", Heat Transfer, Hemisphere Publ. Corp. Washington D. C, Vol 1.

14. Greenberg, J. B. (1986) "A new self-adaptive grid method", AIAA Journal, Vol 23.

15. Hamielec, A. E. and Raal, J. D. (1969) "Numerical studies of viscous flow around circular cylinders", The Physics of Fluids, Vol 12.

16. Hirasaki, G. J. and Hellums, J. D. (1970) "Boundary conditions on the vector and scalar potentials in viscous three dimensional hydrodynamics", Quart. Apl. Maths.

17. Horne, R. N. (1979) "Three dimensional natural convection in a confined porous medium heated from below", J. Fluid Mech., Vol 94.

18 Jain M.K. and Jain R.K. (1987) "Numerical methods for scientific and Engineering computation" .second edition.

19. Jensen, V. G. (1959) "Viscous flow round a sphere at two Reynolds numbers", Proceedings of the Royal Society of London, Series A, Vol 249.

20. Kalugin, V. N. and Panchuk, V.1. (1971) "Viscous incompressible fluid flow along a traveling wave', Hydrodynamic Problems of Bionics, USSR, JPRS 52605.

21. Leonardi, E. (1984) A numerical study of the effects of properties on natural convection", Ph.D. Thesis, The University of New South Wales, Sydney, Australia.

22. Leonardi, E, Reizes, J. A. and de Vahl Davis, (1979) "Natural convection in a rotating annulus", Proc. 2nd Int. Conf. On numerical methods in laminar and turbulent flows.

23. Leonardi, E and Reizes, J. (1981) "Convective flows in closed cavitied with variable properties", Numerical methods in heat transfer, chap. 18, R. W lewis, K. Morgan and O. C Zienkiewicz (eds), John wiley and sons Ltd.

24 Magnus R. and Yoshihara,(1981) "Inviscid transonic flow over airfoils" AIAA Journal, Vol 8.

25. Mallinson, G. D. (1973) "Natural convection in enclosed cavities", ph.D. Thesis, the university of New south wales, Sydney, Australia.

26. Pal, S. (1988) "Grid stretching in finite difference equations", M. E thesis, the university of New South Wales, Sydney, Australia.

27. Pao, Y. H. and Daugherty, R. J. Daugherty, R. J. (1969) "Time-dependent viscous incompressible flow past a finite flat plate", Boeing scientific research laboratories, D1-82-0822.

28. Phillips, R. E. and schmidt F.W. (1984) "Multigrid techniques for numerical solution of diffusion equations", Numerical Heat transfer, Vol 7.

29. Preison, B. C. and Kutler, P. (1980) "Optimal node point distribution for improved accuracy in computational fluid dynamics", AIAA Journal, Vol 18.

30. Samarskii, A.A. (1963) "On a high-accuracy difference scheme for an elliptic equation with several space variables", USSR Comp. Maths and Phys., Vol 3.

31 Sigey S.J. (1988) "Turbulent Natural convection in a rectangular enclosure".M.SC project, Kenyatta University.

32 Stephen M.P. and Victor L.W. (1983) "To compute numerically". Concepts and strategies. Third edition.

33 Skoglund, V. J. and Gay, B. D. (1969) "Improved numerical technique and solution of a separate interaction of an oblique shock wave and a laminar boundary layer", bureau of engineering research report no. Me-41 (69)s-068, the university of New Mexico, Albuqerque, New Mexico.

34 Stella, F. Guj, G. Leonardi, E. Gatheri F.K.and de Vahl Davis, G. 1988 "The velocity/vorticity and vector potential/ vorticity formulation in three dimensional natural convection" UNSW, School of Mech. and Ind. Eng. Report FMT/4.

35. Truesdell, C. (1954) "The Kinematics of Vorticity",Indiana University Press, Bloomington.

36. Wong, A, K. and Reizes, J. A. (1984) "An effective vorticity-vector potential formulation for the numerical solution of 3-D duct flow problems", J. Comp. Phyiscs, Vol 55.

37. Wong, A. K. (1985) "The vector potential in the numerical solution of the Navier-Stokes equations", ph.D. thesis, the university of New South Wales, Sydney Australia.

38. Woods, L. C. (1954) "A note on the numerical solution Vol 5.

39 Yang, H. Q. Tang, K.T. and Lloyd, J. R. (1988) "Three dimensional bimodal buoyant flow transition in tilted enclosures," Int. J. Heat and Fluid Flow, Vol 9.